Topics in Localized Pattern Formation

Michael J. Ward (UBC)

PIMS-Heidelberg: Math-Bio/PDE Workshop

Collaborators:, A. Lindsay (Notre Dame), A. Bernoff (Harvey Mudd), Jia Gou (UMinn, UC Riverside), Sarafa Iyaniwura (UBC).

Outline

- **Topic I:** Berg-Purcell Problem Revisited. Determination of effective capacitance of a sphere with N small "traps" on the boundary. The homogenized limit and the mean first capture time. (Lindsay, Bernoff)
- **Topic II:** PDE/ODE Model of dynamically-active (ODE) small signalling compartments coupled by bulk-diffusion (PDE). Leads to the triggering of (synchronous) oscillations via a hopf bifurcation (J. Gou, S. Iyaniwura). Biologically: illustrates quorum and diffusion sensing behavior.

Key Features: Derivation and study of new discrete variational problems using from Green's interaction matrices.. Nonlinear matrix eigenvalue problems involving Green's interaction matrices.

Topic I: Narrow Capture in 3-D

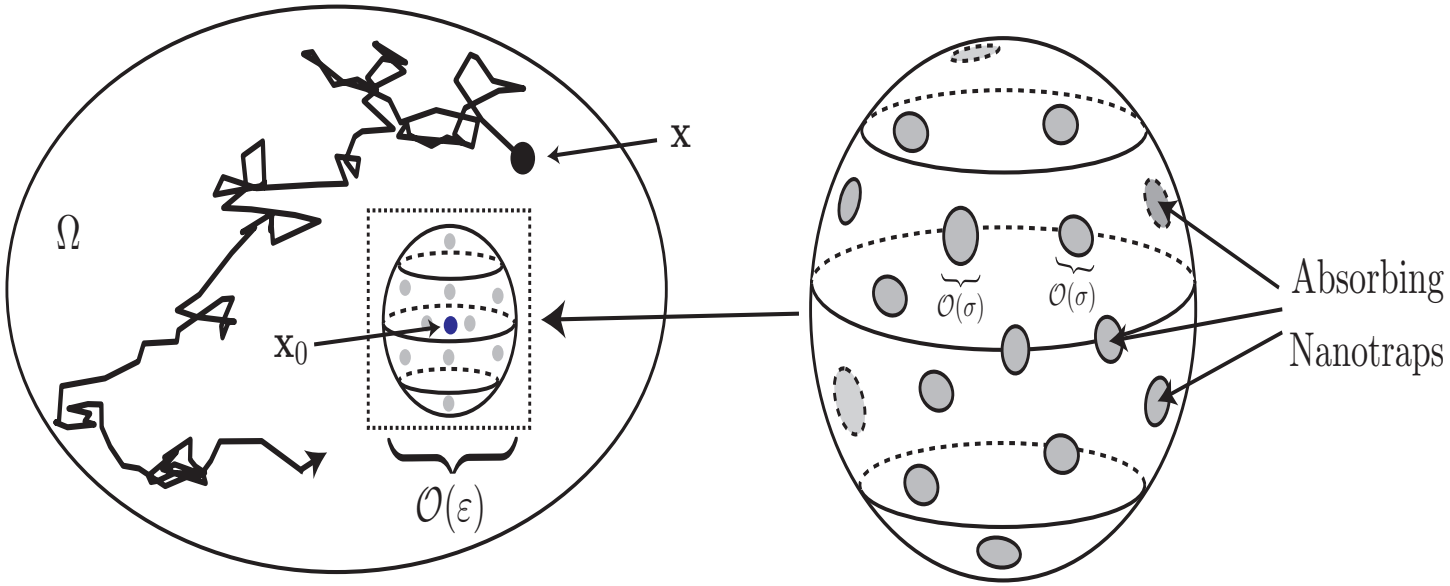

Caption: spherical target of radius $\varepsilon \ll 1$ centered at $\mathbf{x}_0 \in \Omega$, with N locally circular absorbing surface nanotraps (nanopores) of radii $\sigma \ll \varepsilon$ modeled by homogeneous Dirichlet condition.

- A particle (protein etc..) undergoes Brownian walk ($dX_t = DdW_t$) until captured by one of the N small absorbing surface nanotraps.
- Q1: How long on average does it take to get captured? (MFPT).
- Q2: What is the effect on the MFPT of the spatial distribution $\{\mathbf{x}_1, \ldots, \mathbf{x}_N\}$ of the surface nanotraps? (Capacitance).

Applications of Narrow Capture

Nuclear Pores: Genetic material enters nucleus via small pores.

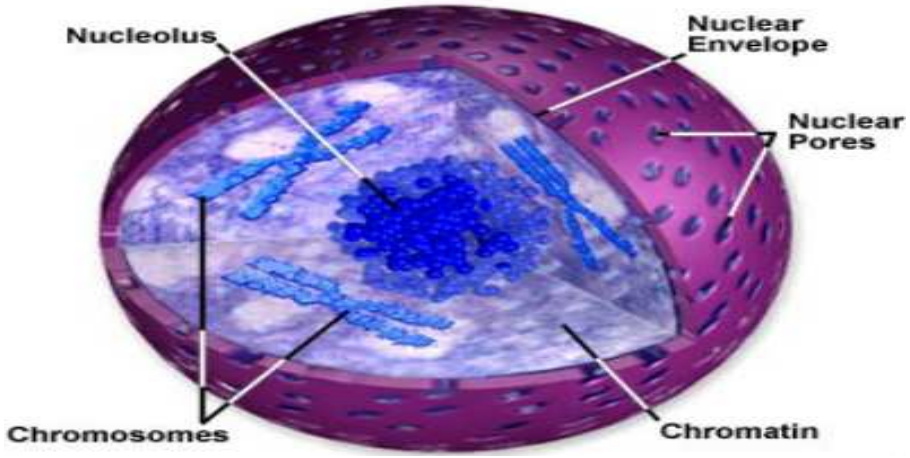

Scaling: Nucleus $\approx 10\%$ of cell volume ($\varepsilon = 0.1$). Roughly, $N = 2000$ pores that occupy 2% of the surface area. (Eilenberg et al. Science 341(6146), 2013).

Cell Signalling: How long does it take an antigen to bind to a receptor on a T-cell to produce antibodies?

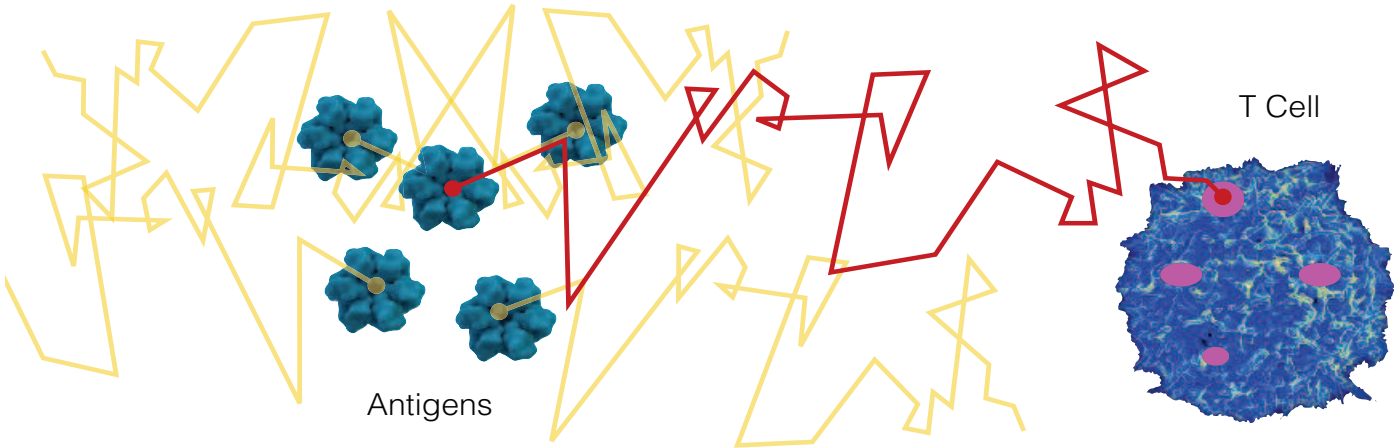

The MFPT PDE for Narrow Capture

The Mean First Passage Time (MFPT) T satisfies

$$\Delta T = -\frac{1}{D}\,, \quad \mathbf{x} \in \Omega \backslash \Omega_{\mathcal{E}}\,; \qquad \partial_n T = 0\,, \quad \mathbf{x} \in \partial\Omega\,,$$
$$T = 0\,, \quad \mathbf{x} \in \partial\Omega_{\mathcal{E}a}\,; \quad \partial_n T = 0\,, \quad \mathbf{x} \in \partial\Omega_{\mathcal{E}r}\,,$$

where $\partial\Omega_{\mathcal{E}a}$ and $\partial\Omega_{\mathcal{E}r}$ are the absorbing and reflecting part of the surface of the small sphere $\Omega_{\mathcal{E}}$ within the 3-D cell Ω.

- Calculate the averaged MFPT $\bar{T}$ for capture of a Brownian particle.
- $\bar{T}$ depends on the capacitance C_0 of the structured target (related to the Berg-Purcell problem, 1977). This is the inner or local problem.
- Derive new discrete optimization problems characterizing the optimal MFPT and determine how the fragmentation of the trap set affects $\bar{T}$.

Ref: [LBW2017] Lindsay, Bernoff, MJW, *First Passage Statistics for the Capture of a Brownian Particle by a Structured Spherical Target with Multiple Surface Traps*, SIAM Multiscale Mod. and Sim. **15**(1), (2017), pp. 74–109.

Asymptotic Result for the Average MFPT

Using strong localized perturbation theory, for $\varepsilon \to 0$ the average MFPT is

$$\bar{T} \equiv \frac{1}{|\Omega \backslash \Omega_\varepsilon|} \int_{\Omega \backslash \Omega_\varepsilon} T \, d\mathbf{x} = \frac{|\Omega|}{4\pi C_0 D \varepsilon} \left[1 + 4\pi \varepsilon C_0 R(\mathbf{x}_0) + \mathcal{O}(\varepsilon^2) \right],$$

where $R(\mathbf{x}_0)$ is the regular part of the Neumann Green's function for Ω:

$$\Delta G = \frac{1}{|\Omega|} - \delta(\mathbf{x} - \mathbf{x}_0), \quad \mathbf{x} \in \Omega; \quad \partial_n G = 0, \quad \mathbf{x} \in \partial\Omega,$$

$$G(\mathbf{x}; \mathbf{x}_0) = \frac{1}{4\pi |\mathbf{x} - \mathbf{x}_0|} + R(\mathbf{x}_0), \quad \text{as} \quad \mathbf{x} \to \xi; \qquad \int_\Omega G \, d\mathbf{x} = 0.$$

Capacitance Problem: "exterior" problem in potential theory. C_0 satisfies

$$\Delta v = 0, \quad \mathbf{y} \in \mathbb{R}^3 \setminus \Omega_0; \quad v = 0, \quad \mathbf{y} \in \Gamma_a, \quad \partial_n v = 0, \quad \mathbf{y} \in \Gamma_r,$$

$$\lim_{R \to \infty} \int_{\partial \Omega_R} \partial_n v \, ds = -4\pi; \quad v \sim -\frac{1}{C_0} + \frac{1}{|\mathbf{y}|} + \mathcal{O}(|\mathbf{y}|^{-2}), \quad |\mathbf{y}| \to \infty.$$

Capacitance C_0 of Structured Target

The inner problem for the capacitance C_0 is equivalent to finding the probability $w(\mathbf{y})$ that a particle is captured starting at $\mathbf{y} \in \mathbb{R}^3 \setminus \Omega_0$:

$$\Delta w = 0\,, \quad \mathbf{y} \in \mathbb{R}^3 \setminus \Omega_0 \text{ (outside unit ball)}$$

$$w = 1\,, \quad \mathbf{y} \in \Gamma_a \text{ (absorbing pores)}$$

$$\partial_n w = 0\,, \quad \mathbf{y} \in \Gamma_r \text{ (reflecting surface)}$$

$$w \sim \frac{C_0}{|\mathbf{y}|} + \mathcal{O}\left(\frac{1}{|\mathbf{y}|^2}\right)\,, \quad \text{as} \quad |\mathbf{y}| \to \infty\,.$$

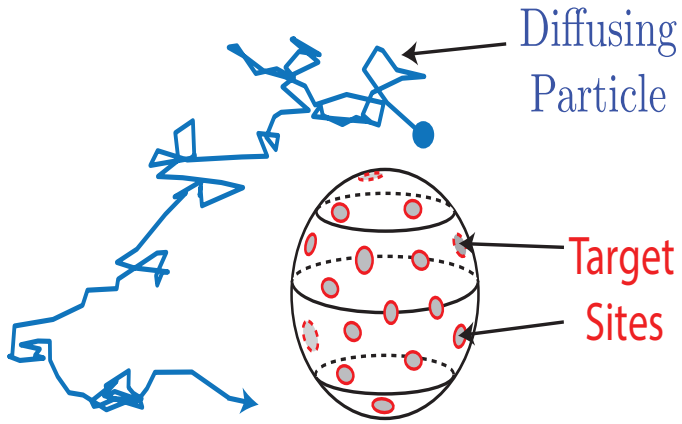

Remarks:

- $C_0 = 1$ if entire surface is absorbing.
- The diffusive flux J into the sphere is

$$J = D \int_{\Gamma_a} \partial_n w \, dS = 4\pi D C_0\,.$$

- The sub-inner problem near a pore is the classic electrified disk problem.

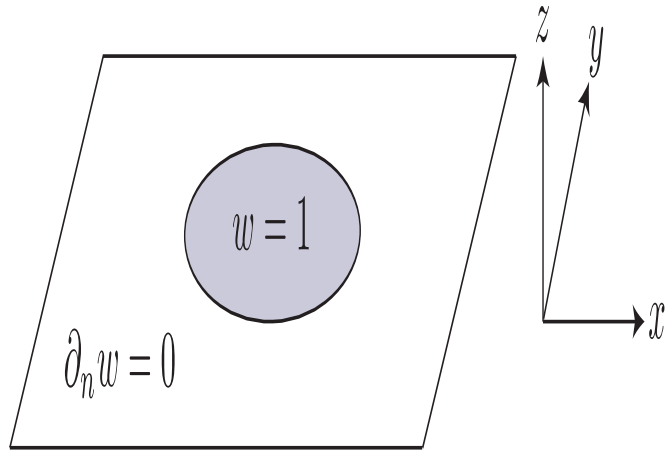

Berg-Purcell Problem: I

This is the Berg-Purcell (BP) problem (Physics of Chemoception, Biophysics, **20**(2), (1977)) ≈ 1500 citations)

BP assumed

- $N \gg 1$ disjoint equidistributed small pores.
- common pore radius $\sigma \ll 1$.
- dilute fraction limit, i.e. $f \equiv N\sigma^2/(4\pi) \ll 1$.

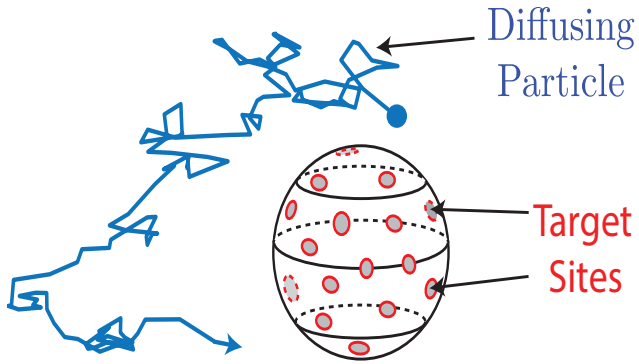

Using a "physically-isnpired" derivation, BP postulated that

$$C_{0\text{bp}} = \frac{N\sigma}{N\sigma+\pi}\,, \qquad J_{\text{bp}} = 4\pi D\frac{N\sigma}{N\sigma+\pi} = 4DN\sigma + \mathcal{O}(\sigma^2)\,.$$

Suggests that J is proportional to the total pore perimeter when $\sigma \ll 1$.

Our Goal: Calculate C_0, and the flux J, systematically for a collection of disjoint pores centered at $\{\mathbf{y}_1, \ldots, \mathbf{y}_N\}$ over the surface. Study the effect of the location of the pores and fragmentation. For equidistributed pores derive the BP result and the asymptotic corrections to it.

Berg-Purcell Problem: II

BP analysis revisited by Shoup-Szabo (Biophysical J. 1982). Replace trap set by effective trapping parameter k, so that for a sphere of radius R

$$\Delta u = 0\,, \quad r \geq R\,; \quad Du_r = ku\,, \quad r = R\,.$$

Then, the flux $J = \int_\Omega D\partial_u r|_{r=R}$ into the sphere is $J = 4\pi DC$, where

$$u = 1 - \frac{C}{r}\,, \quad \text{with} \quad \frac{1}{C} = \frac{1}{R} + \frac{D}{kR^2}\,.$$

Now estimate k: On an infinite plane with a single trap of radius a

$$J_{\text{disk}} = \int_{\text{disk}} Du_z|_{z=0}\, d\boldsymbol{x} = 2\pi D c_{\text{disk}}\,, \qquad c_{\text{disk}} = \frac{2a}{\pi}\,.$$

Thus $J_{\text{disk}} = k_{\text{disk}} = 4aD$. Now estimate

$$k \approx k_{\text{disk}}\left(\frac{N}{4\pi R^2}\right) = \frac{4D}{\pi R\sigma} f\,, \quad \text{where} \quad f \equiv \frac{N\pi\sigma^2}{4\pi}$$

and $\sigma \equiv a/R$. Finally, this yields the BP capacitance and BP flux

$$\frac{1}{C_{\text{bp}}} = \frac{1}{R}\left(\frac{\pi}{N\sigma} + 1\right)\,, \qquad J_{\text{bp}} = 4\pi DR\left(\frac{N\sigma}{N\sigma + \pi}\right)\,.$$

Main Result for C_0 and flux J: I

Main Result: For $\sigma \to 0$, [LBW2017] derived that

$$\frac{1}{C_0} = \frac{\pi}{N\sigma}\left[1 + \frac{\sigma}{\pi}\left(\log\left(2e^{-3/2}\sigma\right) + \frac{4}{N}\mathcal{H}(\mathbf{y}_1,\ldots,\mathbf{y}_N)\right) + \mathcal{O}(\sigma^2\log\sigma)\right],$$

$$J = 4DN\sigma\left[1 + \frac{\sigma}{\pi}\log(2\sigma) + \frac{\sigma}{\pi}\left(-\frac{3}{2} + \frac{2}{N}\mathcal{H}(\mathbf{y}_1,\ldots,\mathbf{y}_N)\right) + \cdots\right]^{-1}.$$

The interpore interaction energy $\mathcal{H}$, subject to $|\mathbf{y}_j| = 1\ \forall j$, is

$$\mathcal{H}(\mathbf{y}_1,\ldots,\mathbf{y}_N) \equiv \sum_{j=1}^{N}\sum_{k=j+1}^{N} g(|\mathbf{y}_j - \mathbf{y}_k|); \quad g(\mu) \equiv \frac{1}{\mu} + \frac{1}{2}\log\mu - \frac{1}{2}\log(2+\mu).$$

Here $\mathbf{y}_j$ for $j = 1,\ldots,N$ are the nanopore centers with $|\mathbf{y}_j| = 1$.

Remarks:

- Flux J minimized when $\mathcal{H}$ minimized
- $g(\mu)$ is monotone decreasing, positive, and convex.
- Indicates that optimal configuration should be (roughly) equidistributed.

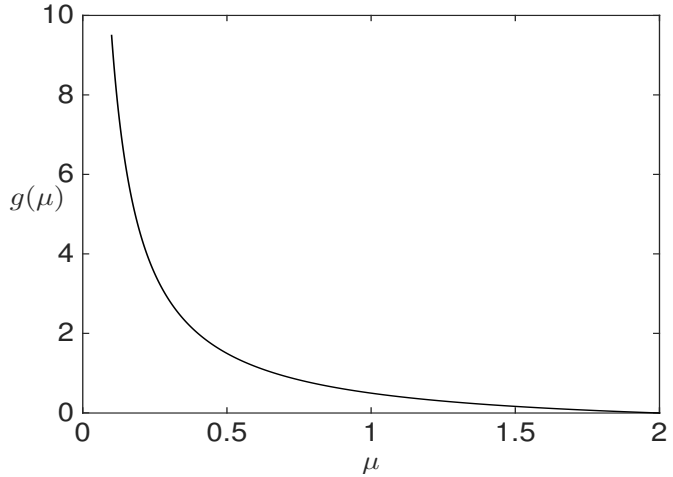

Main Result for C_0 and flux J: II

Here $g(|\mathbf{y}_j - \mathbf{y}_k| = 2\pi G_s(\mathbf{y}_j;\mathbf{y}_k)$, G_s is the surface-Neumann G-function

$$G_s(\mathbf{y}_j;\mathbf{y}_k) = \frac{1}{2\pi}\left[\frac{1}{|\mathbf{y}_j - \mathbf{y}_k|} - \frac{1}{2}\log\left(\frac{1 - \mathbf{y}_j\cdot\mathbf{y}_k + |\mathbf{y}_j - \mathbf{y}_k|}{|\mathbf{y}_j| - \mathbf{y}_j\cdot\mathbf{y}_k}\right)\right].$$

Key steps in singular perturbation analysis for C_0:

- Asymptotic expansion of global (outer) solution and local (inner) solutions near each pore (using tangential-normal coordinates).
- The surface G_s-function has a subdominant logarithmic singularity on the boundary (related to surface diffusion). This fact requires adding "logarithmic switchback terms in σ" in the outer expansion.
- The leading-order local solution is the tangent plane approximation and yields electrified disk problem in a half-space, with (local) capacitance $c_j = 2\sigma/\pi$.
- **Key:** Need corrections to the tangent plane approximation in the inner region near the pore. This higher order term in the inner expansion satisfies a Poisson-type problem, with monopole far-field behavior.
- Asymptotic matching and solvability conditions yield $1/C_0$.

Asymptotics versus Numerics (Small N)

Asymptotic Results: For $\sigma \to 0$

$$J = 4D\sigma \left[1 + \frac{\sigma}{\pi}\left(\log(2\sigma) - \frac{3}{2}\right) - \frac{\sigma^2}{\pi^2}\left(\frac{\pi^2 + 21}{36}\right) + \cdots\right], \quad (N = 1),$$

$$J = 4DN\sigma \left[1 + \frac{\sigma}{\pi}\log(2\sigma) + \frac{\sigma}{\pi}\left(-\frac{3}{2} + \frac{2}{N}\mathcal{H}(\mathbf{y}_1, \ldots, \mathbf{y}_N)\right) + \cdots\right]^{-1}, \quad (N > 1).$$

Numerics: Compare with full numerics from multipole theory based on integral equations [Bernoff, Lindsay]. **Vertices at Platonic Solids.**

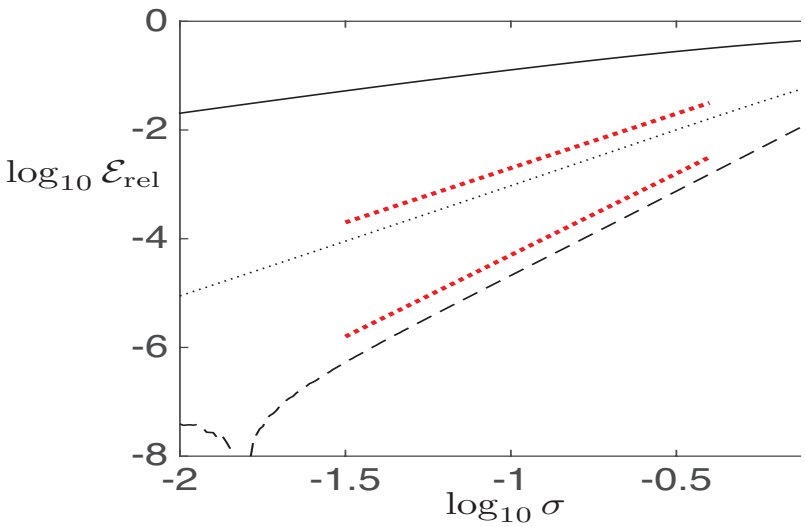

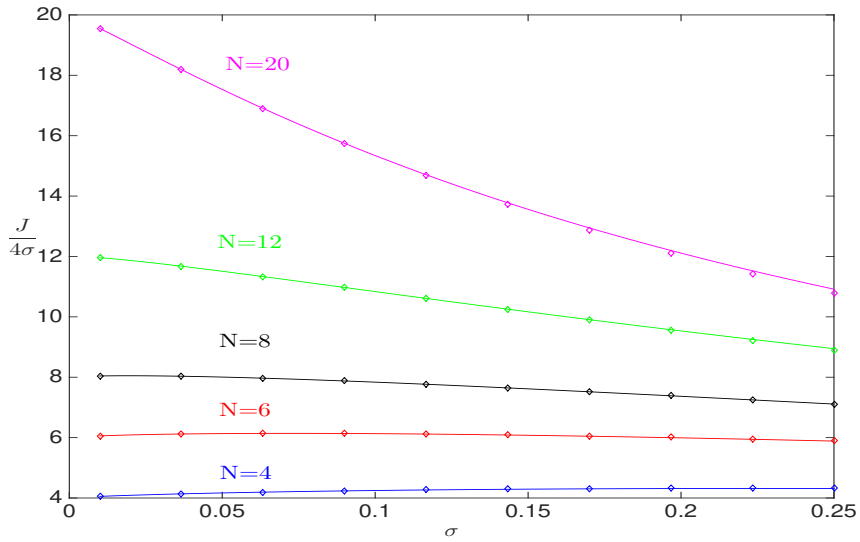

Left: One pore: log-log plot of relative error. Leading-order (solid), three-term (dotted), four-term (dashed). **Right:** Comparison of rescaled flux $J/(4\sigma)$ versus σ when pores are centered at vertices of platonic solids. Marked points are full numerics.

Clustering and Fragmenting the Pore Set

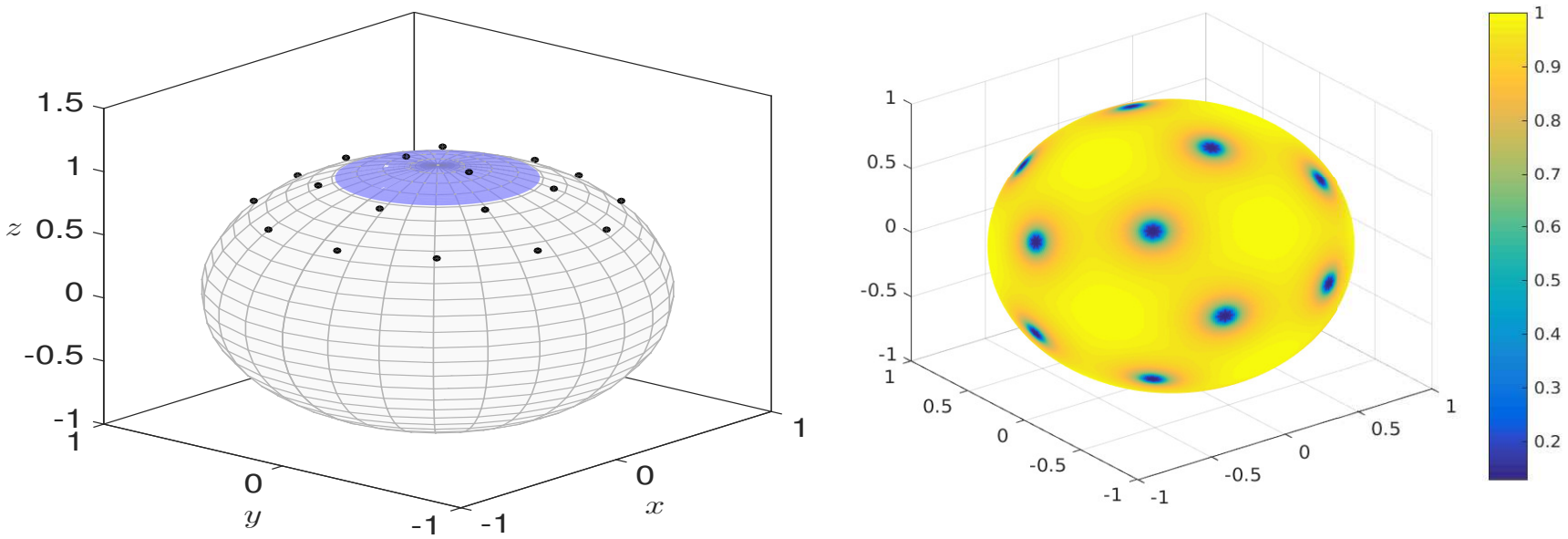

Left: $N = 20$ equally-spaced nanopores (centers shown only) clustered in the polar region $\theta \in (0, \frac{\pi}{3})$ with total absorbing fraction $f = 0.05$. Blue pore: is the equivalent area as a single nanopore. Nanopore radius is $\sigma = 2\sqrt{f/N}$. Right: optimal dodecahedron pattern.

$$\frac{1}{C_0} \approx 5.41 \ \text{(single Pore)}\,; \quad \frac{1}{C_0} \approx 2.79 \ \text{(clustered)}; \quad \frac{1}{C_0} \approx 1.98 \ \text{(optimal)}\,.$$

Conclude I: subdividing a single nanopore into 20 smaller, but clustered, nanopores of same total area rougly halves the MFPT to the target.

Conclude II: The MFPT for 20 optimally distributed pores is significantly smaller than for 20 clustered pores.

Discrete Energy: Equidistributed Points

Find global minimum $\mathcal{H}_{\min}$ of $\mathcal{H}$ when $N \gg 1$

$$\mathcal{H} = \sum_j \sum_{k \neq j} g(|\mathbf{y}_j - \mathbf{y}_k|), \quad \text{where} \quad g(\mu) \equiv \frac{1}{\mu} + \frac{1}{2} \log\left(\frac{\mu}{2+\mu}\right).$$

- What is asymptotics of $\mathcal{H}_{min}$ as $N \to \infty$?
- For large N, many local minima, so finding global min is difficult.
- Cannot tile a spherical surface with hexagons (must have defects).
- Related to classic Fekete point problems of minimizing pure Coulombic energies on the sphere (Smale's 7th problem).

Three Coverings of $N = 800$ points

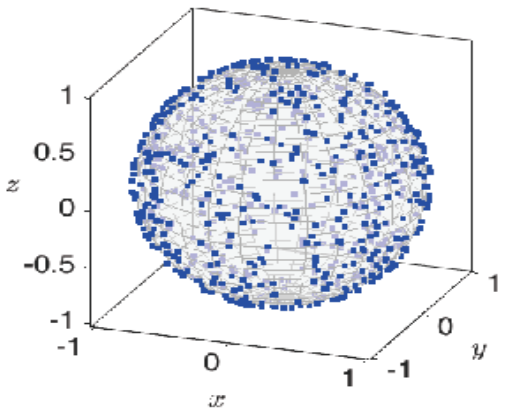

Uniform Random
Not Great

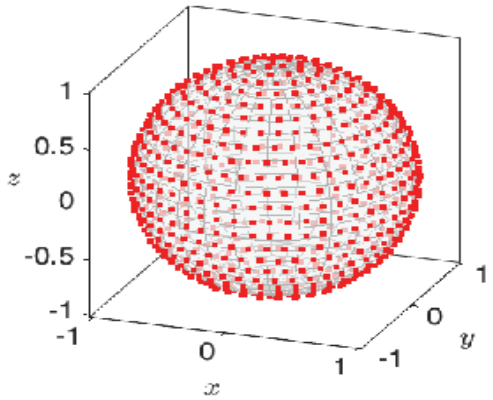

Equispaced in (θ, ϕ)
Better

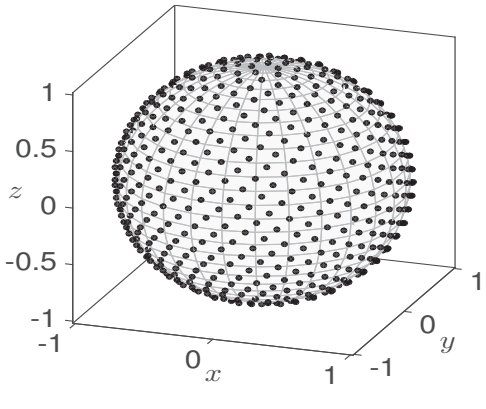

Fibonacci Spirals
Best (so far...)

Scaling Law: Equidistributed Points

Formal Large N Limit: For N large and "equidistributed points", we have

$$\mathcal{H}_{min} \sim \frac{N^2}{4} - d_1 N^{3/2} + \frac{N}{8}\log N + d_2 N + d_3 N^{1/2} + \cdots,$$

with $d_1 = 1/2$, $d_2 = 1/8$ and $d_3 = 1/4$. Better to use $d_1 = 0.55230$ for "pure" Coulombic interactions [Saff].

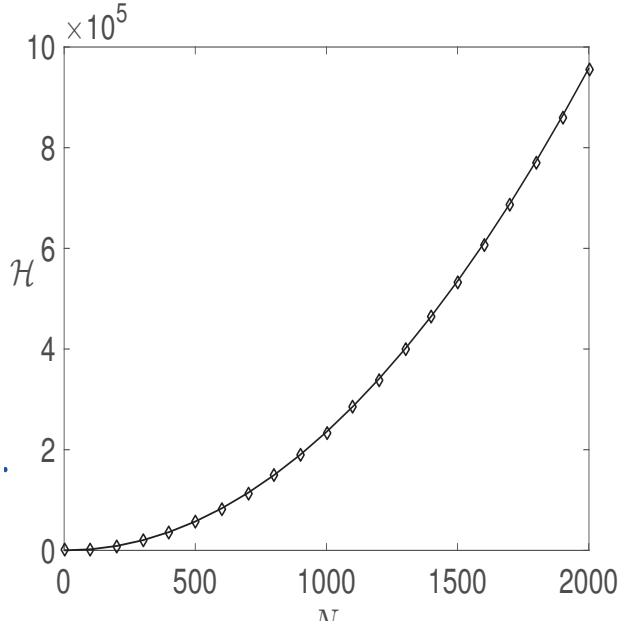

Main Result (Scaling Law): For $N \gg 1$, but small pore surface area fraction $f = \mathcal{O}(\sigma^2 \log \sigma)$ and with equidistributed pores, the optimal C_0 and J are

$$\frac{1}{C_0} \sim 1 + \frac{\pi\sigma}{4f}\left(1 - \frac{8d_1}{\pi}\sqrt{f} + \frac{\sigma}{\pi}\log\left(\beta\sqrt{f}\right) + \frac{2d_3\sigma^2}{\pi\sqrt{f}}\right), \quad \beta \equiv 4e^{-3/2}e^{4d_2},$$

$$J \sim 4\pi D\left[1 + \frac{\pi\sigma}{4f}\left(1 - \frac{8d_1\sqrt{f}}{\pi} + \frac{\sigma}{\pi}\log\left(\beta\sqrt{f}\right) + \frac{2d_3\sigma^2}{\pi\sqrt{f}}\right)\right]^{-1}.$$

BP Result is the leading-order term. Our analysis yields correction terms for the sphere. Most notable is the $\sqrt{f}$ term, where $f \equiv N\sigma^2/4$.

Fragmentation Effects

Effect of Fragmentation: fix pore fraction f, increase N, and obtain σ from $f = N\pi\sigma^2/[4\pi]$. Locate pores centered at spiral Fibonacci points.

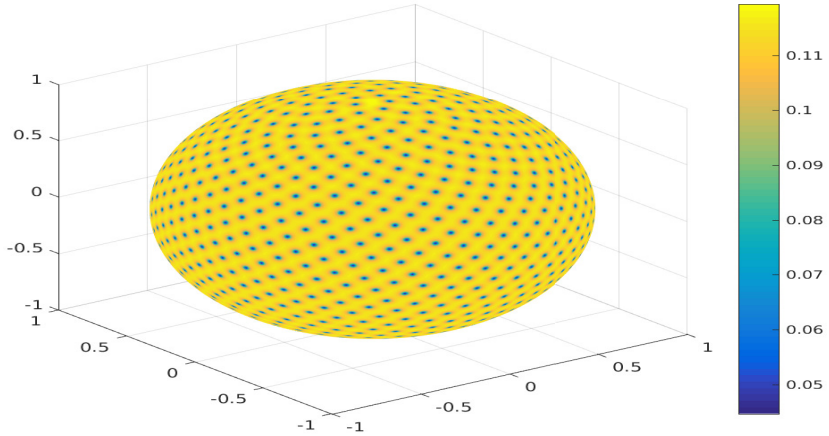

Caption: 1001 Nanopores at vertices of the spiral Fibonacci points.

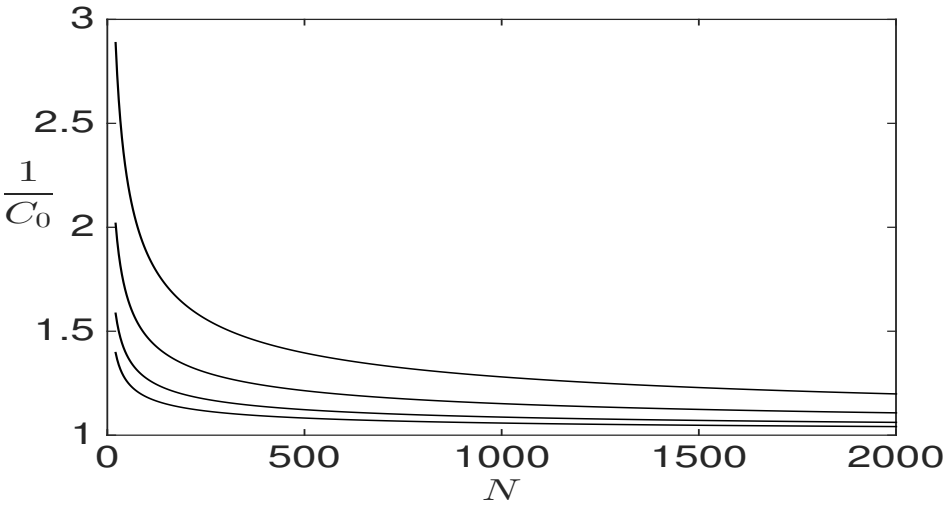

Caption: From top to bottom: $f = \{0.02, 0.05, 0.1, 0.15\}$ For $N = 2000$, $f = 0.02$, full numerics gives $C_{0n}^{-1} = 1.1985$ and $C_0^{-1} = 1.2028$ (scaling law).

Conclusion: Fragmentation effects are significant until N becomes large.

Compare Scaling Law with Full Numerics

Compare full numerics with the asymptotic scaling law

$$J \sim 4\pi D \left[1 + \frac{\pi\sigma}{4f}\left(1 - \frac{8d_1\sqrt{f}}{\pi} + \frac{\sigma}{\pi}\log\left(\beta\sqrt{f}\right) + \frac{2d_3\sigma^2}{\pi\sqrt{f}}\right)\right]^{-1}.$$

Fix 2% pore coverage ($f = 0.02$) and choose spiral Fibonacci points.

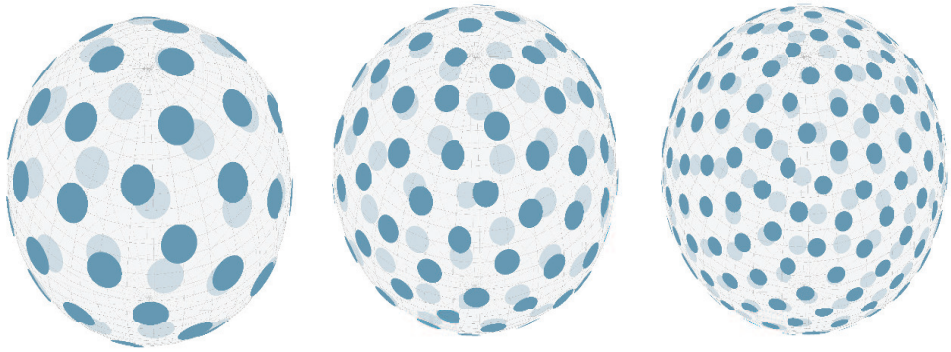

$N = 51$ $N = 101$ $N = 201$

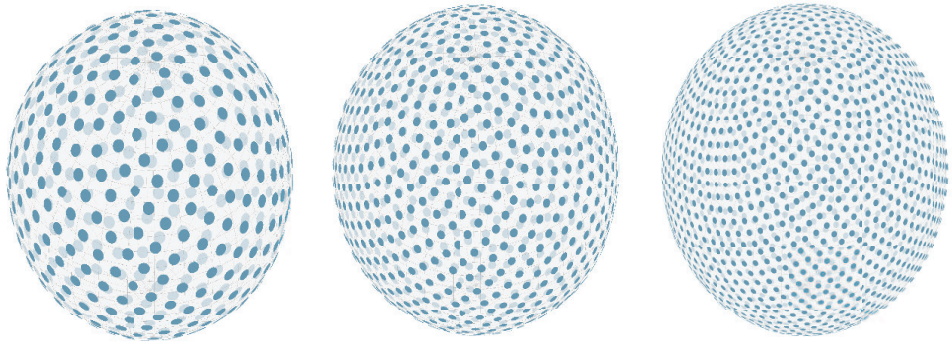

$N = 501$ $N = 1001$ $N = 2001$

N	$\mathcal{E}_{\text{rel}}$
51	1.02%
101	0.90%
201	0.76%
501	0.58%
1001	0.37%
2001	0.34%

Caption: $f = 0.02$ (2% pore coverage). Scaling law accurately predicts the flux to the target for the biological parameters $f = 0.02$ and $N = 2001$.

Effective Robin Condition: Leakage κ_h

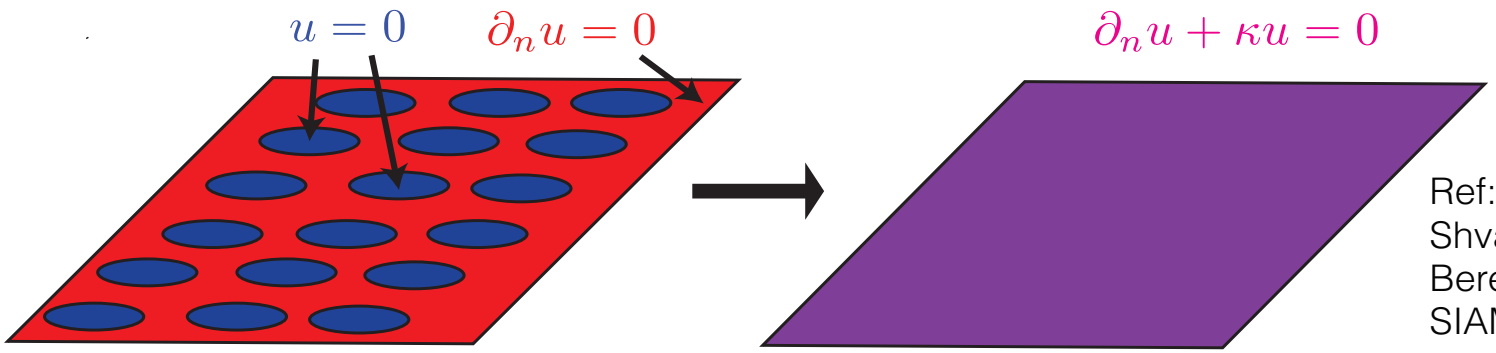

Ref: Muratov, Shvartsmam, Berezhkovskii, SIAM MMS 2006.

Consider the planar case with σ pore radius and f coverage. Previous empirical laws (Berezhkovskii 2013) for a hexagonal arrangement

$$\kappa = \frac{4Df}{\pi\sigma}\chi(f)\,, \qquad \chi(f) = \frac{1 + 1.37\sqrt{f} - 2.59f^2}{(1-f)^2}\,,$$

Our homogenized Robin condition: use scaling law for C_0 and find κ_h from

$$\Delta v_h = 0\,,\ \ |\mathbf{y}| > 1\,;\ \ \partial_n v_h + \kappa_h v_h = 0\,,\ \ |\mathbf{y}| = 1\,;\ \ v_h(\mathbf{y}) \sim \frac{1}{|\mathbf{y}|} - \frac{1}{C_0}\,,\ \ |\mathbf{y}| \to \infty\,.$$

For the unit sphere, and in terms of d_1, d_2, d_3 and $\beta \equiv 4e^{-3/2}e^{4d_2}$, we get

$$\kappa_h \sim \frac{4Df}{\pi\sigma}\left[1 - \frac{8d_1}{\pi}\sqrt{f} + \frac{\sigma}{\pi}\log\left(\beta\sqrt{f}\right) + \frac{2d_3\sigma^2}{\pi\sqrt{f}}\right]^{-1} \approx \frac{4Df}{\pi\sigma}\left[1 + 1.41\sqrt{f} + \cdots\right].$$

Further Directions

- Rigorus results for the large N behavior of $\mathcal{H}$.
- Not just MFPT, but full time-dependent probability density.
- Potential theoretic methods (fast) to compute capacitance (L. Greengard, J. Kaye, preprint archive)
- Derive an explicit formula for the capacitance of a bumpy sphere containing N nanopores
  - Local analysis near a pore is possible, but no explicit globally-defined surface Neumann Green's function.
  - Needed for asymptotics: computation of surface Neumann Green's function and its local behavior near the singularity.
  - Full numerical computations based on integral equations challenging.

Topic II: Active Cells Coupled by Diffusion

Formulate and analyze a model of (ODE) dynamically active small "cells", with arbitrary intracellular kinetics, that are coupled spatially by a linear bulk-diffusion field (PDE) in a bounded 2-D domain.

Specific Questions:

- Can one trigger oscillations in the small cells (Hopf bifurcation), that would otherwise not occur without the coupling via bulk diffusion?
- Can we exhibit quorum sensing behavior by which cells oscillate and synchronize their dynamics when the population reaches a threshold?
  - In terms of the number m of cells per unit area, i.e. cell population density is $\rho = m/|\Omega|$.
  - What parameters regulate this threshold?
  - Usually studied from an ODE approach.
- Can we exhibit diffusion sensing behavior whereby cells oscillate and synchronize their dynamics based on:
  - cell spatial configuration (synchronization easier for clustered cells).
  - magnitude of diffusivity D of extracellular chemical (autoinducer).
  - Requires a PDE-based model.

Dynamical Quorum Sensing in Nature

Collective behavior in “cells” driven by chemical signalling between them.

- Collections of spatially segregated unicellular (eukaryotic) organisms such as starving yeast cells (glycolysis) coupled only through extracellular signalling molecules (autoinducer is Acetaldehyde). **Ref:** De Monte et al., PNAS **104**(47), (2007).
- Amoeba colonies (Dicty) in low nutrient enviroments, with cAMP organizing the aggregation of starving colonies; **Ref:** Nanjundiah, Bio. Chem. **72**, (1998), Gregor et al. Science, **328**, (2010).
- Catalyst bead particles (BZ particles) interacting through a chemical diffusion field; **Ref:** Tinsley, Showalter, et al. “Dynamical Quorum Sensing... Collections of Excitable and Oscillatory Cataytic Particles”, Physica D **239** (2010).

Key Ingredient: Need intracellular autocatalytic signal and an extracellular communication mechanism (bulk diffusion or autoinducer) that influences the autocatalytic growth. In the absence of coupling by bulk diffusion, the “cells” are in a quiescent state. Oscillations and ultimate sychronization occurs via a switchlike response to elevated levels of the autoinducer.

Amoeba Colony (*Dictyostelium discoideum*)

- About 180 cells are confined into an area of 420 μm in diameter (2-D).
- When resources are scarce, each cell secretes cAMP into the medium.
- Main Question: Is the oscillation an intrinsic property of the cells or does it only occur at the population level?

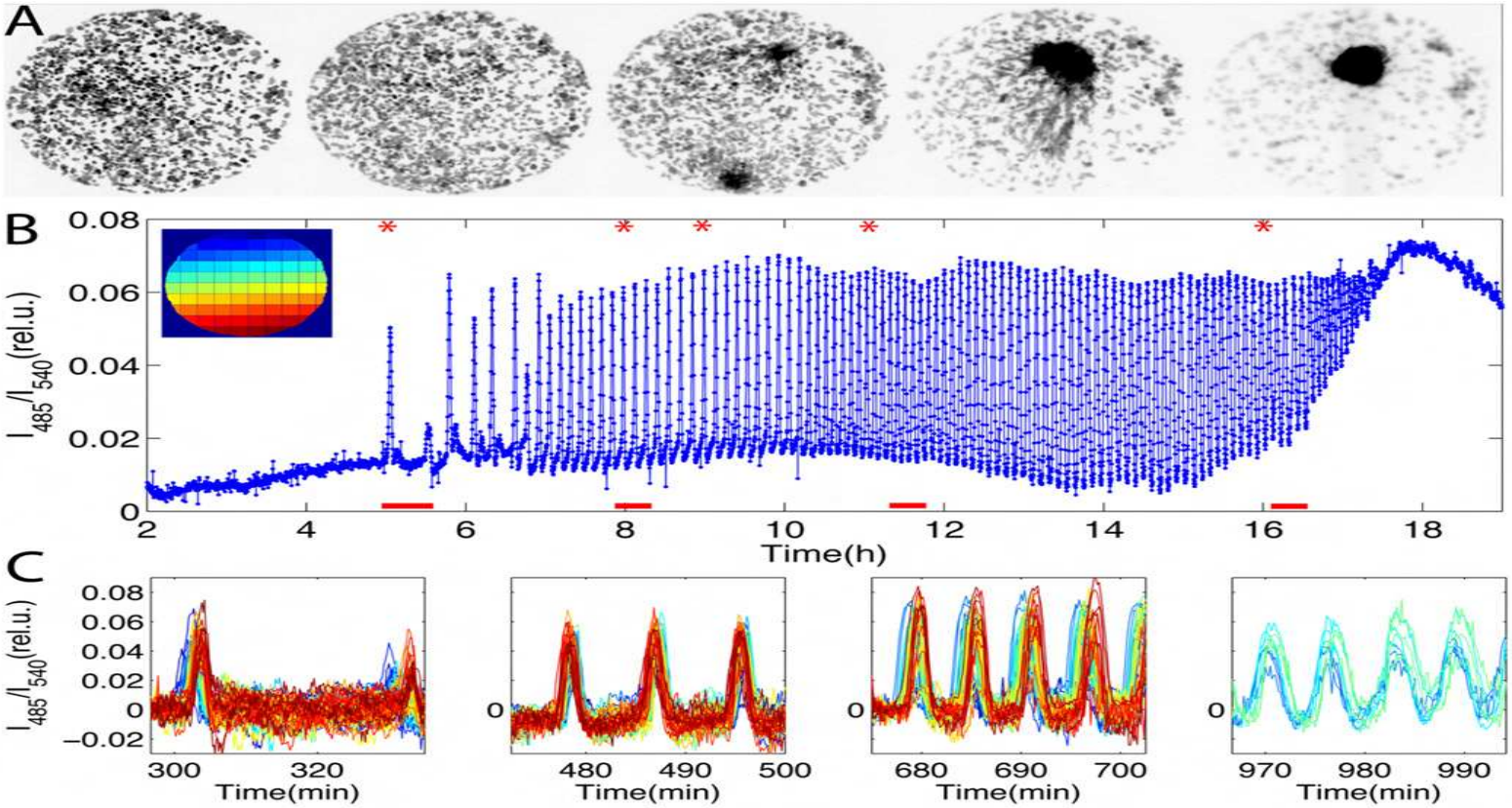

Caption: The cells secrete cAMP into the medium which first initiates a coordinated collective response. On longer time-scale cells aggregate. **Ref:** The Onset of Collective Behavior in Social Amoebae, T. Gregor et al. Science 2010

Modeling Approaches

- **Large ODE system** of weakly coupled system of oscillators. Prototypical is the Kuramoto type-models for the coupled oscillator phases:

$$\frac{d\mathbf{x}_i}{dt} = \mathbf{F}(\mathbf{x}_i) + \sigma \sum_j C_{ij}\mathbf{H}(\mathbf{x}_j)\,,$$

  Synchrony occurs between individual oscillators as the coupling strength σ increases. (Vast literature, but not the mechanism here).

- **Homogenization** approach of deriving RD systems through cell densities: Yields target and spiral wave patterns of cAMP in Dicty modeling (but phemenological).

- **More Recent:** PDE-ODE models coupling individual "cells" through a bulk diffusion field. Our framework related to:
  - **Ref:** J. Muller, C. Kuttler, et al. "Cell-Cell Communication by Quorum Sensing and...", J. Math. Bio. **53** (2006),
  - J. Muller, H. Uecker, J. Math. Bio. **67** (2013). (steady-state analysis in 3-D, dynamics).

Ref [GW]: J. Gou, M.J. Ward, J. Nonlinear Sci., **26**(4), (2016), pp. 979–1029.

Formulation of the 2-D Model: I

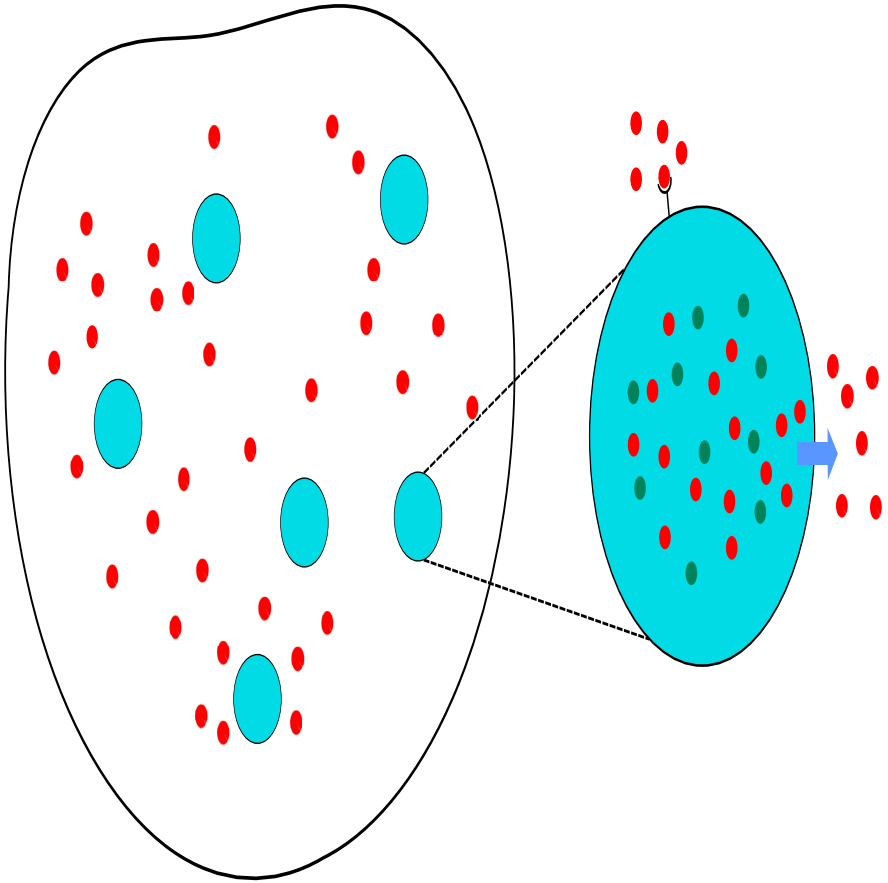

- The m cells are circular and each contains n chemicals $\mu_j = (\mu_{1j}, \ldots, \mu_{nj})^T$. When isolated they interact via ODE's $\mathbf{d}\mu_j/dt = \mathbf{F}_j(\mu_\mathbf{j})$.
- A scalar bulk diffusion field (autoinducer) diffuses in the space between the cells via

$$\mathcal{U}_T = D_B \Delta_\mathbf{X} \mathcal{U} - k_B \mathcal{U} \, .$$

- There is an exchange across the cell membrane, regulated by permeability parameters, between the autoinducer and one intracellular species (Robin condition).

Scaling Limit: $\epsilon \equiv \sigma/L \ll 1$, where L is lengthscale for Ω. We assume that the permeability parameters are $\mathcal{O}(\epsilon^{-1})$.

Parameters: Bulk diffusivity D_B, bulk decay k_B, permeabilities, ϵ, and time-scale of intracellular reactions.

Formulation of the 2-D Model: II

Our PDE-ODE coupled cell-bulk model in 2-D with m cells is

$$\mathcal{U}_T = D_B \Delta_{\boldsymbol{X}} \mathcal{U} - k_B \mathcal{U}\,, \quad \boldsymbol{X} \in \Omega \backslash \cup_{j=1}^{m} \Omega_j\,; \quad \partial_{n_{\boldsymbol{X}}} \mathcal{U} = 0\,, \quad \boldsymbol{X} \in \partial\Omega\,,$$

$$D_B \partial_{n_{\boldsymbol{X}}} \mathcal{U} = \beta_{1j} \mathcal{U} - \beta_{2j} \mu_j^1\,, \qquad \boldsymbol{X} \in \partial\Omega_j\,, \quad j = 1, \ldots, m\,.$$

Each cell $\Omega_j \in \Omega$ is a disk of radius σ centered at some $\boldsymbol{X}_j \in \Omega$.

Inside each cell there are n interacting species with mass vector $\boldsymbol{\mu}_j \equiv (\mu_j^1, \ldots, \mu_j^n)^T$ whose dynamics are governed by n-ODEs, with (rank-one) coupling via integration over the j-th "cell"-membrane $\partial\Omega_j$:

$$\frac{d\boldsymbol{\mu}_j}{dT} = k_R \mu_c \boldsymbol{F}_j\left(\boldsymbol{\mu}_j/\mu_c\right) + \boldsymbol{e}_1 \int_{\partial\Omega_j} \left(\beta_{1j}\mathcal{U} - \beta_{2j}\mu_j^1\right) dS_j\,, \quad j = 1, \ldots, m\,,$$

where $\boldsymbol{e}_1 \equiv (1, 0, \ldots, 0)^T$, and μ_c is typical mass.

- Only one species μ_j^1 can cross the j-th cell membrane into the bulk.
- $k_R > 0$ is intracellular reaction rate; β_{1j}, β_{2j} are permeabilities.
- The dimensionless function $\boldsymbol{F}_j(\boldsymbol{u}_j)$ models the intracellular dynamics.

Formulation of the 2-D Model: III

Dimensionless Formulation: The concentration of signalling molecule $U(\boldsymbol{x},t)$ in the bulk satisfies the PDE:

$$\tau U_t = D\Delta U - U\,, \qquad \boldsymbol{x}\in\Omega\backslash\cup_{j=1}^m\Omega_{\epsilon_j}\,; \quad \partial_n U = 0\,, \quad \boldsymbol{x}\in\partial\Omega\,,$$

$$\epsilon D\partial_{n_j}U = d_{1j}U - d_{2j}u_j^1\,, \qquad \boldsymbol{x}\in\partial\Omega_{\epsilon_j}\,, \quad j=1,\ldots,m\,.$$

The cells are disks of radius $\epsilon \ll 1$ so that $\Omega_{\epsilon_j}\equiv\{\boldsymbol{x}\,|\,|\boldsymbol{x}-\boldsymbol{x}_j|\le\epsilon\}$.

Inside each cell there are n interacting species $\boldsymbol{u}_j=(u_j^1,\ldots,u_j^n)^T$, with intracellular dynamics for each $j=1,\ldots,m$,

$$\frac{d\boldsymbol{u}_j}{dt} = \boldsymbol{F}_j(\boldsymbol{u}_j) + \frac{\boldsymbol{e}_1}{\epsilon\tau}\int_{\partial\Omega_{\epsilon_j}}(d_{1j}U - d_{2j}u_j^1)\,ds\,, \qquad \boldsymbol{e}_1\equiv(1,0,\ldots,0)^T\,.$$

Remark: The time-scale is measured wrt intracellular reactions. The dimensionless bifurcation parameters are: d_{1j}, d_{2j} (permeabilities); τ (reaction-time ratio); D (effective diffusivity);

$$\tau\equiv\frac{k_R}{k_B}\,, \quad D\equiv\left(\frac{\sqrt{D_B/k_B}}{L}\right)^2\,, \quad \beta_{1j}\equiv(k_BL)\,\frac{d_{1j}}{\epsilon}\,, \quad \beta_{2j}\equiv\left(\frac{k_B}{L}\right)\frac{d_{2j}}{\epsilon}\,.$$

Theoretical Framework

- Can one trigger oscillations in the small cells, via a Hopf bifurcation, that would otherwise not be present without the coupling via bulk diffusion? (i.e. each cell is a conditional oscillator). Intuition: Need reaction-time ratio τ in some interval $0 < \tau_- < \tau < \tau_+ < \infty$.
- Can we exhibit quorum sensing and diffusion sensing behavior?

Two key regimes for D with different behaviors:

- $D = \mathcal{O}(1)$; Effect of spatial distribution of cells is a key factor whether oscillations are triggered or not (diffusion sensing behavior).
- $D \gg \mathcal{O}(\nu^{-1})$; In this "well-mixed" regime, the PDE-ODE cell-bulk model reduces to a finite dimensional dynamical system with global coupling. Quorum sensing behavior observed.

Mathematical Framework: Use strong localized perturbation theory (SLPT) to construct steady-states, to formulate the linear stability problem, and to derive the limiting well mixed ODE system.

Steady-States: Matched Asymptotics

Main Result (Steady-State): *In the outer region, the ss bulk diffusion field is*

$$U(\boldsymbol{x}) = -2\pi \sum_{i=1}^{m} S_i G(\boldsymbol{x}, \boldsymbol{x}_i)\,, \quad \text{where} \quad \boldsymbol{S} \equiv (S_1, \ldots, S_m)^T .$$

In terms of $\nu = -1/\log\epsilon$ *and a Green's matrix* $\mathcal{G}$*, we obtain a nonlinear algebraic system for* $\boldsymbol{S}$ *and* $\boldsymbol{u}^1 \equiv \left(u_1^1, \ldots, u_m^1\right)^T$*, where* $e_1 = (1, 0, \ldots, 0)^T$*:*

$$\boldsymbol{F}_j(\boldsymbol{u}_j) + \frac{2\pi D}{\tau} S_j \boldsymbol{e}_1 = 0\,, \quad (\mathcal{H} + 2\pi\nu\mathcal{G})\,\boldsymbol{S} = -\nu\mathcal{W}\boldsymbol{u}^1\,, \quad j = 1, \ldots, m\,.$$

Here $\mathcal{W} \equiv \text{diag}\left(\frac{d_{21}}{d_{11}}, \ldots, \frac{d_{2m}}{d_{1m}}\right)$ and $\mathcal{H} \equiv \text{diag}\left(\left(1 + \frac{\nu D}{d_{11}}\right), \ldots, \left(1 + \frac{\nu D}{d_{1m}}\right)\right)$.

In this ss formulation, the entries of the $m \times m$ Green's matrix $\mathcal{G}$ are

$$(\mathcal{G})_{ii} = R_i\,, \qquad (\mathcal{G})_{ij} = G(\boldsymbol{x}_i; \boldsymbol{x}_j)\,, \quad i \neq j\,,$$

where, with $\varphi_0 \equiv 1/\sqrt{D}$, $G(\boldsymbol{x}; \boldsymbol{x}_j)$ is the reduced-wave G-function:

$$\Delta G - \varphi_0^2 G = -\delta(\boldsymbol{x} - \boldsymbol{x}_j)\,, \quad \boldsymbol{x} \in \Omega\,; \qquad \partial_n G = 0\,, \quad \boldsymbol{x} \in \partial\Omega\,.$$

$$G(\boldsymbol{x}; \boldsymbol{x}_j) \sim -\frac{1}{2\pi}\log|\boldsymbol{x} - \boldsymbol{x}_j| + R_j + o(1)\,, \qquad \text{as} \quad \boldsymbol{x} \to \boldsymbol{x}_j\,.$$

Globally Coupled Eigenvalue Problem (GCEP)

Main Stability Result: *For $\epsilon \to 0$, the perturbed bulk diffusion field satisfies*

$$u(\boldsymbol{x},t) = U(\boldsymbol{x}) + e^{\lambda t}\eta(\boldsymbol{x})\,, \qquad \eta(\boldsymbol{x}) = -2\pi \sum_{i=1}^{m} c_i G_\lambda(\boldsymbol{x},\boldsymbol{x}_i)\,.$$

Inside the j-th cell we have $\boldsymbol{u}_j = \boldsymbol{u}_{ej} + 2\pi D\tau^{-1} c_j e^{\lambda t}(\lambda I - J_j)^{-1}\boldsymbol{e}_1$. Here $\boldsymbol{c} = (c_1,\ldots,c_m)^T$ is a nullvector of the GCEP:

$$\mathcal{M}\boldsymbol{c} = \boldsymbol{0}\,, \qquad \mathcal{M}(\lambda) \equiv 2\pi\nu\mathcal{G}_\lambda + \mathcal{H} + \nu\frac{2\pi D}{\tau}\mathcal{W}\mathcal{K}(\lambda)\,.$$

In this GCEP, $\mathcal{G}_\lambda$ is the Green's matrix formed from

$$\Delta G_\lambda - \varphi_\lambda^2 G_\lambda = -\delta(\boldsymbol{x}-\boldsymbol{x}_j), \quad \boldsymbol{x}\in\Omega\,; \qquad \partial_n G_\lambda = 0\,, \quad \boldsymbol{x}\in\partial\Omega\,,$$

$$G_\lambda(\boldsymbol{x};\boldsymbol{x}_j) \sim -\frac{1}{2\pi}\log|\boldsymbol{x}-\boldsymbol{x}_j| + R_{\lambda,j} + o(1)\,, \qquad \text{as} \quad \boldsymbol{x}\to\boldsymbol{x}_j\,,$$

with $\varphi_\lambda \equiv D^{-1/2}\sqrt{1+\tau\lambda}$. Here $\mathcal{K}$ is the diagonal matrix defined in terms of the Jacobian $J_j \equiv \boldsymbol{F}_{j,\boldsymbol{u}}(\boldsymbol{u}_{ej})$ of the intracellular kinetics $\boldsymbol{F}_j$:

$$\mathcal{K}_j = \boldsymbol{e}_1{}^T(\lambda I - J_j)^{-1}\boldsymbol{e}_1 = \frac{M_{j,11}(\lambda)}{\det(\lambda I - J_j)}\,, \quad \text{where} \quad e_1 = (1,0,\ldots,0)^T\,.$$

Numerics for the GCEP

Linear stability analysis: Nonlinear matrix eigenvalue problem of the form

$$\mathcal{M}(\lambda;\tau,D)\boldsymbol{c}=\mathbf{0}\,.$$

Definition: An unstable "mode" is a root λ of $\mathcal{F}(\lambda)=\det\left(\mathcal{M}(\lambda)\right)=0$ in $\mathrm{Re}(\lambda)>0$. The number N of unstable modes is the total number of such roots. The eigenvector $\boldsymbol{c}$ determines the amplitude and phase at each cell.

- Determine N numerically from winding number computation of $\mathcal{F}(\lambda)$ over a large semi-circle in $\mathrm{Re}(\lambda)>0$. Gives a "stability map" in (τ,D) plane with $N=0$ (white), $N=2$ (grey), $N=4$ (blue), etc..
- Hopf bifurcation boundaries, $\lambda=i\lambda_I(D)$ and $\tau=\tau(D)$ can have folds in D. Compute with $\mathrm{Re}\mathcal{F}=0$ and $\mathrm{Im}\mathcal{F}=0$ using psuedo-arclength.

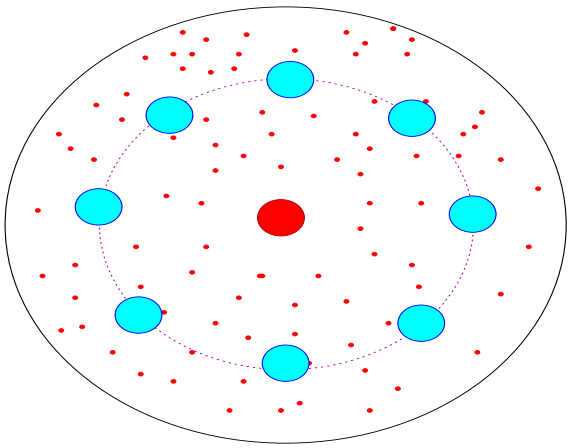

Tractable: Ring and Ring + Center Hole Pattern:

- Small identical cells inside unit disk, evenly spaced on a concentric ring of radius r_0.
- The center-cell can have different kinetics, or different permeabilities d_1 and d_2.
- Matrix spectrum $\mathcal{M}\boldsymbol{c}=\sigma\boldsymbol{c}$ available analytically.

Intracellular Selkov Reaction-Kinetics

Selkov Kinetics: Let $\boldsymbol{u} = (u_1, u_2)^T$ be intracellular dynamics given by Selkov model (used for modeling glycolysis oscillations):

$$F_1(u_1, u_2) = \alpha u_2 + u_2 u_1^2 - u_1\,, \quad F_2(u_1, u_2) = \epsilon_0 \left(\mu - (\alpha u_2 + u_2 u_1^2)\right)\,.$$

For an *isolated cell* $\exists$ a unique steady-state at $u_{1e} = \mu$, $u_{2e} = \mu/(\alpha + \mu^2)$. The determinant and trace of the Jacobian J_e is

$$\text{trace}(J_e) = \frac{\left[\mu^2 - \alpha^2 - \epsilon_0(\alpha + \mu^2)^2\right]}{\alpha + \mu^2}\,, \quad \det(J_e) = \varepsilon_0(\alpha + \mu^2) > 0\,.$$

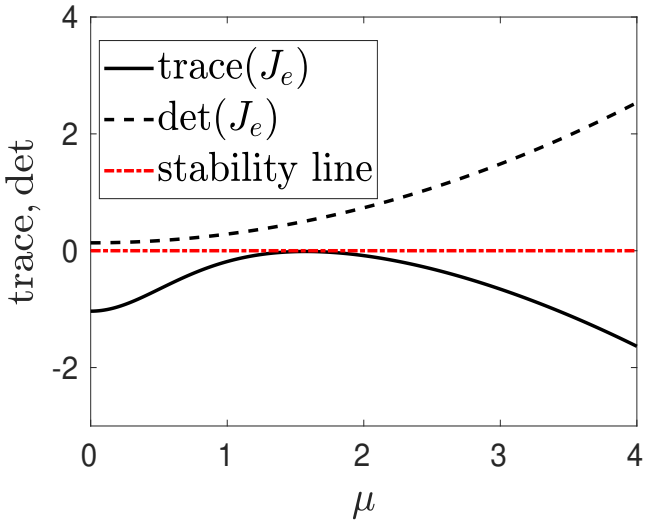

- **Fix Selkov parameters** as $\alpha = 0.9$, and $\epsilon_0 = 0.15$ and plot versus μ.
- For $\mu = 2$ an isolated cell has a stable fixed point with no oscillations, but is near to stability threshold.

Remark: When coupled to the other cells there is a new (but unique) steady-state and the PDE-ODE coupling can trigger oscillations via a HB.

$D = \mathcal{O}(1)$: Ring Patterns

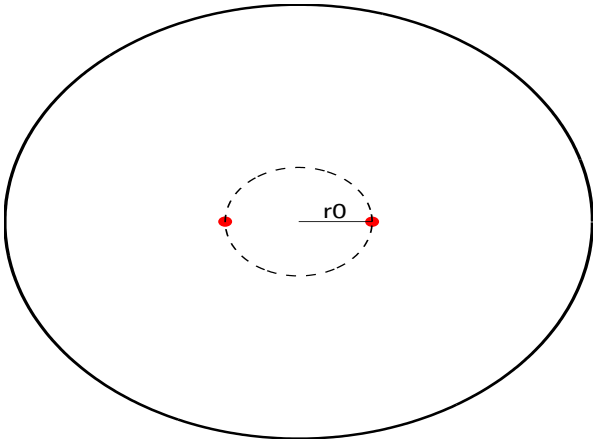

Analytically Tractable Example:

- m small cells inside the unit disk, evenly spaced on a concentric ring of radius r_0.
- Assume identical kinetics and permeabilities, so that $\boldsymbol{F}_j = \boldsymbol{F}$, $d_{1j} = d_1$, and $d_{2j} = d_2$.

Spectral Problem (from GCEP): *Must find the roots λ to $\mathcal{B}_j(\lambda) = 0$, where*

$$\mathcal{B}_j(\lambda) \equiv \omega_{\lambda,j} + \frac{1}{2\pi\nu}\left(1 + \frac{D\nu}{d_1}\right) + \left(\frac{d_2 D}{d_1 \tau}\right)\frac{M_{11}}{\det(\lambda I - J)}\,, \qquad j = 1, \ldots, m\,.$$

Here $\omega_{\lambda,j}$ are the eigenvalues of the λ-dependent Green's matrix $\mathcal{G}_\lambda$:

$$\mathcal{G}_\lambda \boldsymbol{v}_j = \omega_{\lambda,j}\boldsymbol{v}_j\,, \qquad j = 1, \ldots, m\,,$$

- $\exists$ a steady-state with $S_j = S_c$ for all $j = 1, \ldots, m$.
- $\mathcal{G}_\lambda$ and $\mathcal{G}$ are symmetric, cyclic matrices. Hence $\boldsymbol{v}_1 = (1, \ldots, 1)^T$ (synchronous mode).
- For the unit disk, the Green's matrix $\mathcal{G}_\lambda$ is given analytically in terms of an infinite series of modified Bessel functions of complex argument.

$D = \mathcal{O}(1)$: Ring Patterns: II

Linear Stability Computations (Theory):

- **Phase Diagram:** Compute Hopf Bifurcation (HB) boundaries in the τ versus D plane for each $j = 1, \ldots, m$ by setting $\lambda = i\lambda_I$. Fix r_0, $\epsilon = 0.05$, $d_1 = 0.8$, and $d_2 = 0.2$.
- **Winding Number** computations used to check where $\mathrm{Re}(\lambda) > 0$ in open regions of the τ versus D plane.
- **Cyclic Symmetric Matrices:**: Matrix spectrum of $\mathcal{G}_\lambda$ readily calculated. Note: $\boldsymbol{v}_1 = \boldsymbol{e} \equiv (1, \ldots, 1)^T$ (synchronous mode), while $\boldsymbol{e}^T \boldsymbol{v}_j = 0$ for $j = 2, \ldots, m$ are the asynchronous modes. However, mode degeneracy occurs due to cyclicity and symmetry of $\mathcal{G}_\lambda$. In particular, if $m = 5$, there are exactly two asynchronous branches.

Qualitative Questions: What is the effect of:

- cell clustering (i.e. smaller r_0?)
- the cell permeabilities d_1 and d_2?
- the number m of cells?
- small changes in the intracellular kinetics?

$D = \mathcal{O}(1)$: HB Boundaries: $m = 2$ Cells

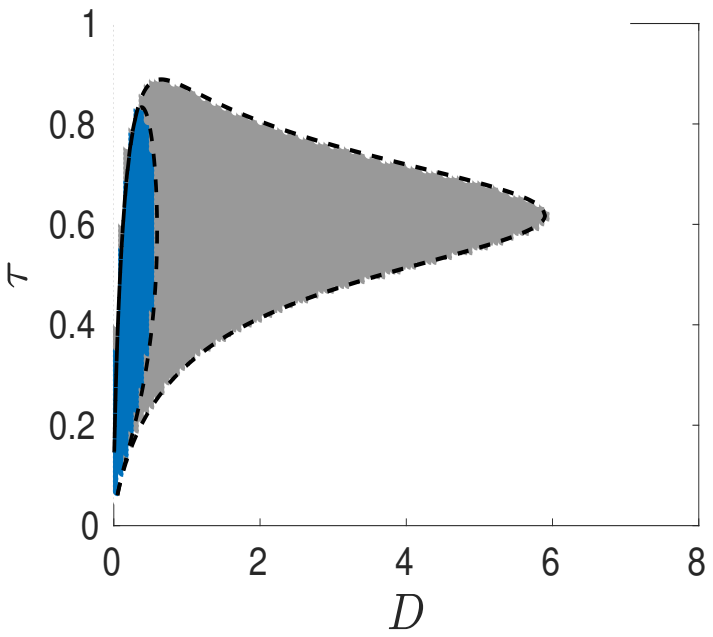

- HB boundaries τ vs. D for $m = 2$ and $r_0 = 0.75$.
- Synchronous and asynchronous HB boundaries (heavy dashed).
- $N = 2$ (grey) and $N = 4$ (blue). (winding-number results)
- Asynchronous lobe exists only for D small.
- Predicts no oscillations for $D \gg 1$.

Numerical Validation: FlexPDE for a similar map with $r_0 = 0.25$

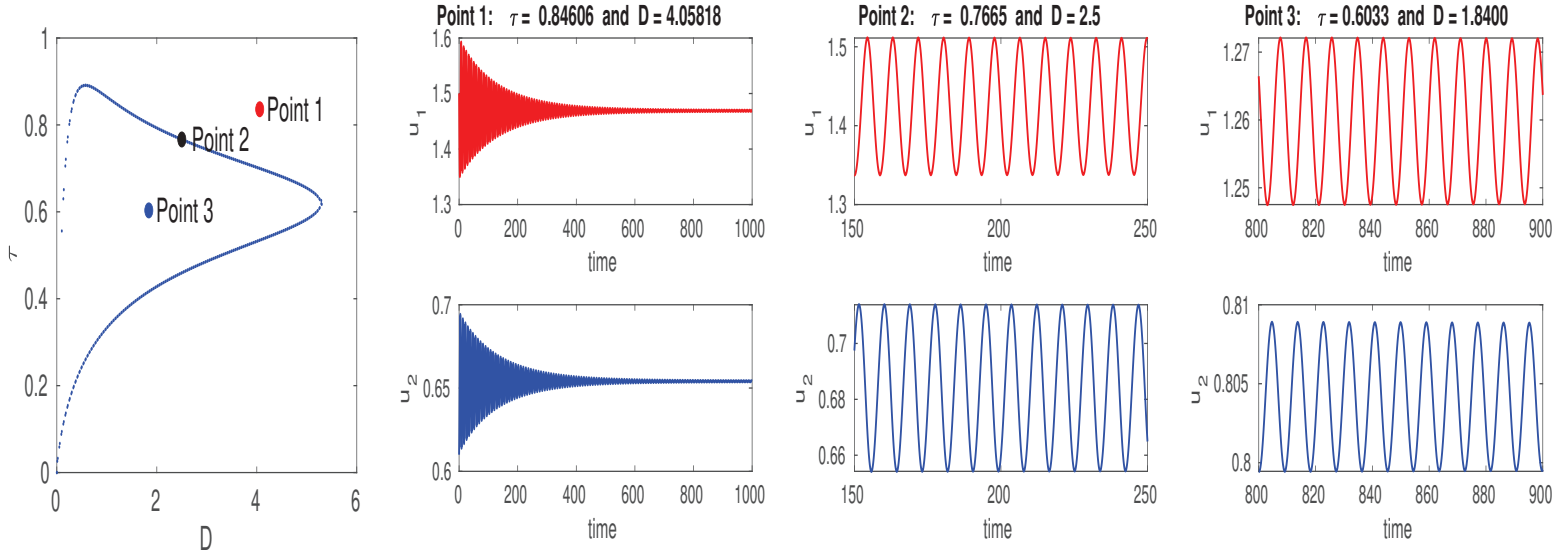

$D = \mathcal{O}(1)$: Diffusion Sensing Behavior

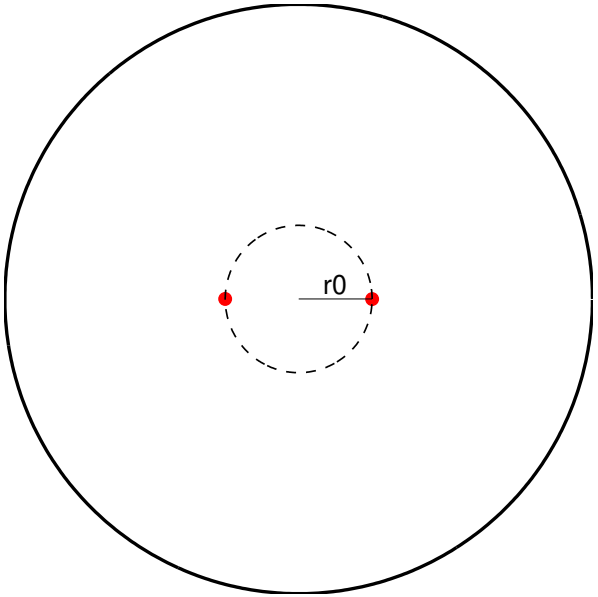

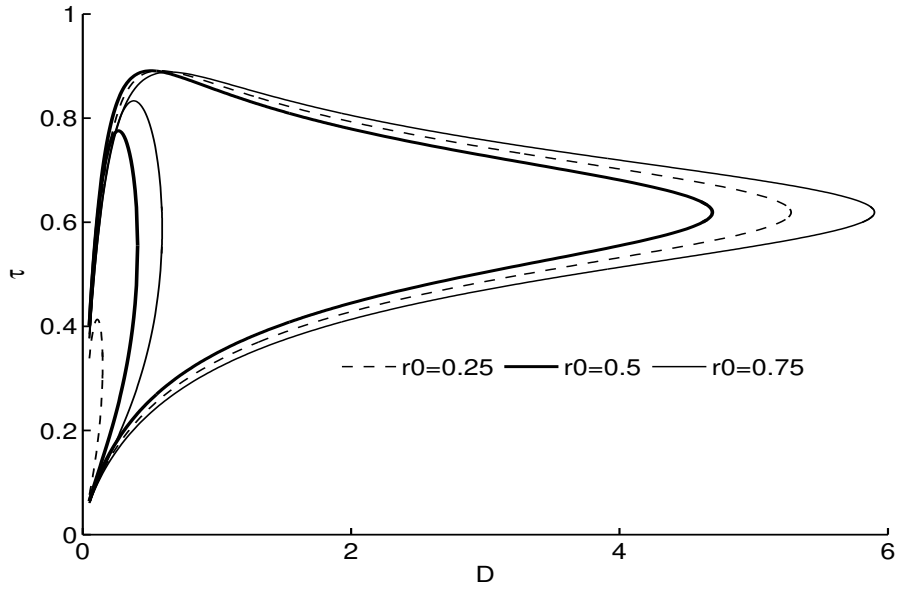

Caption: Let $m = 2$ and vary r_0: HB boundaries in τ versus D for the synchronous mode (larger lobes) and the asynchronous mode (small lobes for D small).

- Asynchronous lobe is smallest when $r_0 = 0.25$ (i.e. for closely-spaced cells). Implies that D has to be only increased a bit before asynchronous oscillations are impossible.
- If $r_0 = 0.75$ the two cells are rather close to their images across the boundary of the disk (Neumann BC).
- Diffusion sensing: If $D = 5$ and $\tau = 0.6$, we are outside instability lobe for $r_0 = 0.5$ but within the lobes for $r_0 = 0.25$ and $r_0 = 0.75$. Thus a more clustered configuration will trigger oscillations for the same D.

$D = \mathcal{O}(1)$: HB Boundaries $m = 5$

HB boundaries: $m = 5$ cells and $r_0 = 0.5$.(Right is zoom of left)

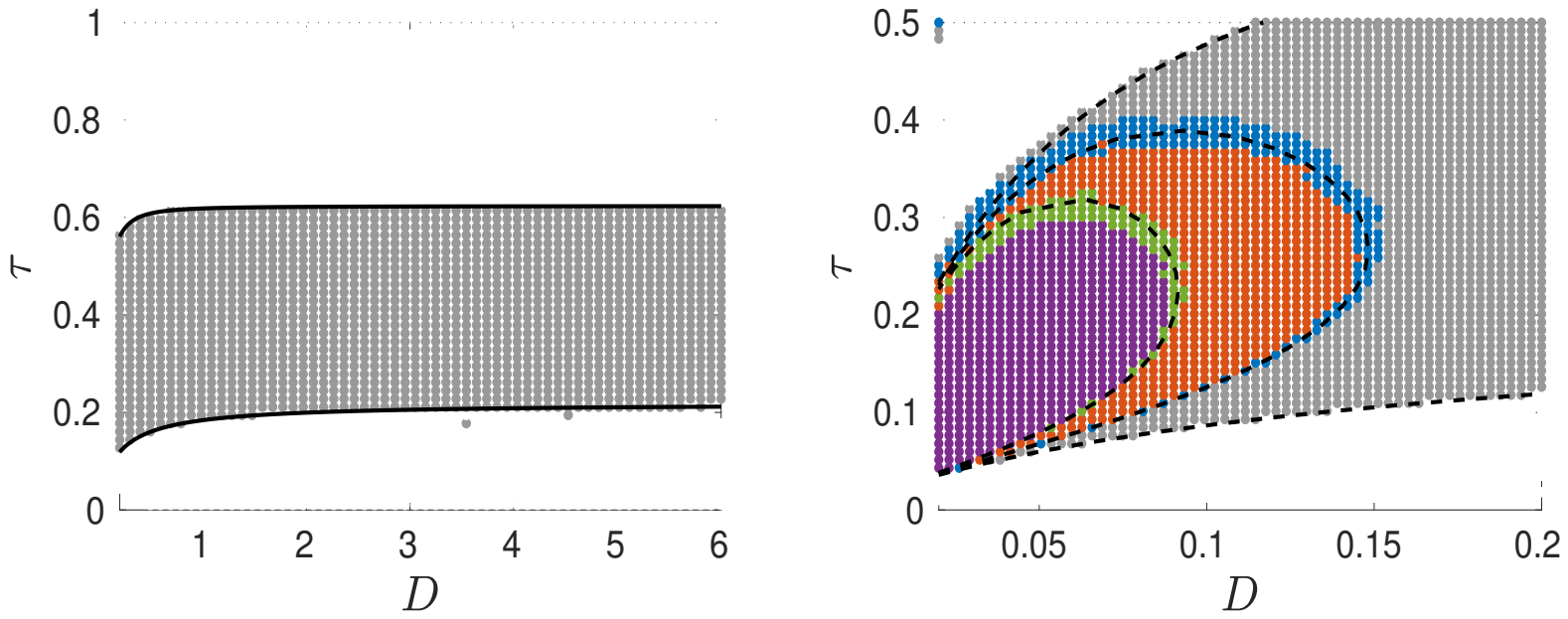

- $N = 2$ (grey), $N = 6$ (red), $N = 10$ (cyan).
- Asynchronous lobes: only for D small. Two such lobes when $m = 5$.
- Instability lobe for synchronous mode is now unbounded (left figure).

Implication: The unbounded lobe for the synchronous mode indicates that for the well-mixed limit $D \to \infty$ a Hopf bifurcation for the steady-state will occur when $\tau = \tau_{\pm}$ (horizontal asymptotes), and that an oscillatory instability occurs for $\tau_- < \tau < \tau_+$.

Ring + Center Pattern: Role of Permeability

Consider $m = 5$ with a defective cell at the center of the disk with different permeabilities than four identical cells on a ring of radius $r_0 = 0.75$.

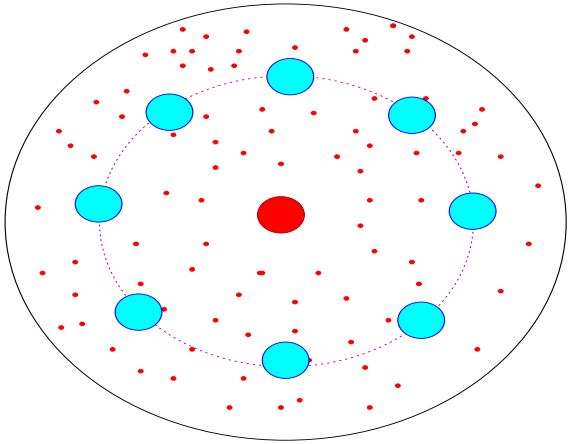

- **Ring Cells:** $d_1 = 0.8$, $d_2 = 0.2$ (identical kinetics)
- **Center Cell: Case I:** $d_1 = 0.8$, $d_2 = 0.2$. **Case II (Defective):** $d_1 = 0.4$, $d_2 = 0.2$.
- $\mathcal{M}$ is a 5×5 symmetric matrix with a 4×4 cyclic block with the fifth row being (b, b, b, b, r).

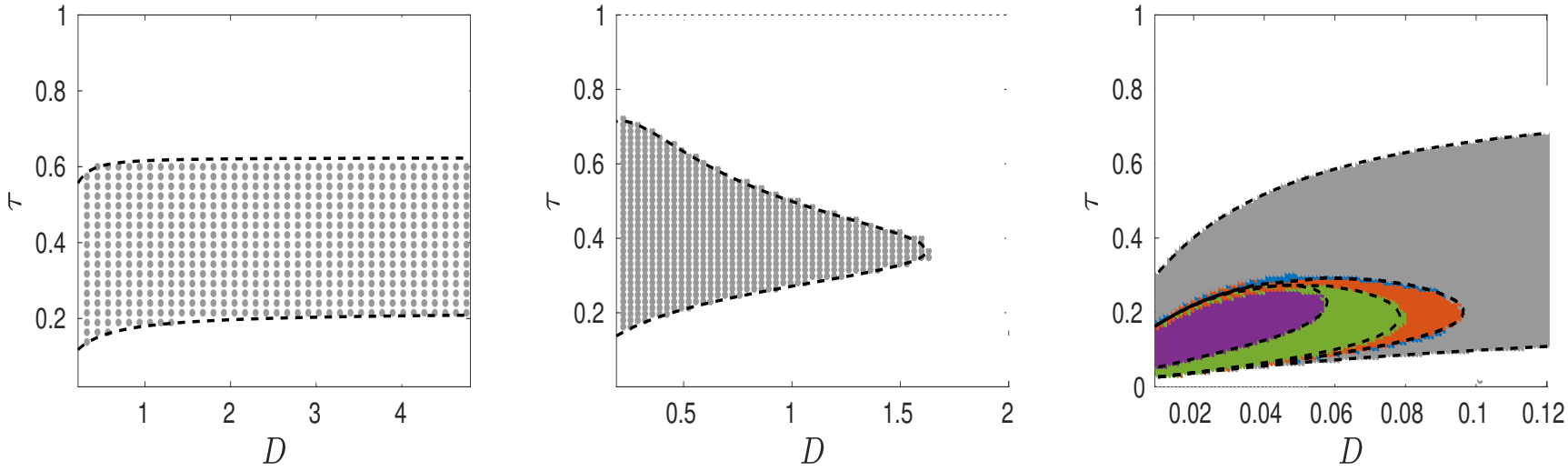

Caption: Left: **Case I:** all identical. Middle: **Case II:** center defective. Right: Zoom for small D with $N = 0$ (white), $N = 2$ (grey), $N = 4$ (blue), $N = 6$ (red), $N = 8$ (green), $N = 10$ (cyan).

Ring + Center Pattern: A Triggering Center Cell

Consider $m = 5$ with a defective cell at the center of the disk that has a different intracellular kinetic (Selkov) parameter closer to stability threshold of an isolated cell than the four identical cells on the ring.

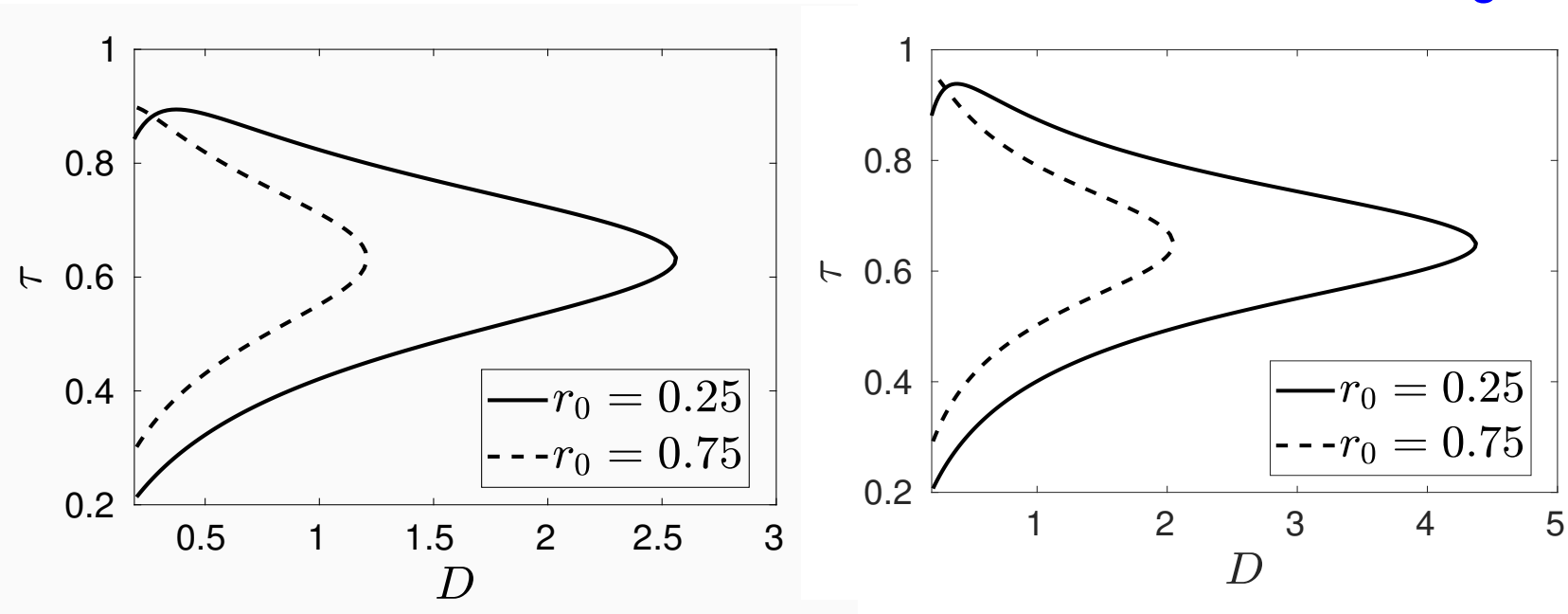

Caption: Lobes of instability for the synchronous mode $\boldsymbol{c} = (1, 1, 1, \xi)$: Left: all identical cells $d_1 = 0.3$, $d_2 = 0.2$, $\alpha = 0.9$. Right: center-cell has $\alpha = 0.86$.

- Small change in intracellular kinetics can have large effect on region in τ versus D parameter space where oscillations occur.
- With more clustering $(r_0 = 0.25)$, one can have a larger bulk diffusivity D before autoinducer wanders too far from cells to trigger collective behavior.

The Well-Mixed Regime $D \gg \mathcal{O}(\nu^{-1})$: I

Goal: Derive and analyze a reduced finite-dimensional dynamical system characterizing the cell-bulk interations from PDE-ODE system for $D \to \infty$.

An asymptotic analysis yields that in the bulk that $u(x,t) \sim U_0(t)$, where

$$U_0' = -\frac{1}{\tau} U_0 - \frac{\rho}{\tau} \left(\frac{1}{m} \sum_{j=1}^{m} \left[\kappa_{1,j} U_0 - \kappa_{2,j} u_j^1 \right] \right) ,$$

$$\boldsymbol{u}_j' = \boldsymbol{F}_j(\boldsymbol{u}_j) + \frac{1}{\tau} \left[\kappa_{1,j} U_0 - \kappa_{2,j} u_j^1 \right] \boldsymbol{e}_1 , \qquad j = 1, \ldots, m ,$$

where $\boldsymbol{e}_1 = (1, 0, \ldots, 0)^T$. Here ρ is the effective cell density and

$$\rho \equiv \frac{m}{|\Omega|} , \qquad \kappa_{1,j} \equiv 2\pi d_{1,j} , \qquad \kappa_{2,j} \equiv 2\pi d_{2,j} .$$

Large system of ODEs with weak but global coupling when $0 < d_{1j} << 1$ and $0 < d_{2j} \ll 1$, or when $\tau \gg 1$.

Identical Cells: Look for $\boldsymbol{u}_j = \boldsymbol{u}$, $\forall j$. We get

$$U_0' = -\frac{1}{\tau} \left(1 + \kappa_1 \rho \right) U_0 + \rho \frac{\kappa_2}{\tau} u_1 , \qquad \boldsymbol{u}' = \boldsymbol{F}(\boldsymbol{u}) + \frac{1}{\tau} \left[\kappa_1 U_0 - \kappa_2 u_1 \right] \boldsymbol{e}_1 .$$

The Well-Mixed Regime $D \gg \mathcal{O}(\nu^{-1})$: II

Selkov with $d_1 = 0.8$, $d_2 = 0.2$ and $|\Omega| = \pi$. Global Bifurcation Study.

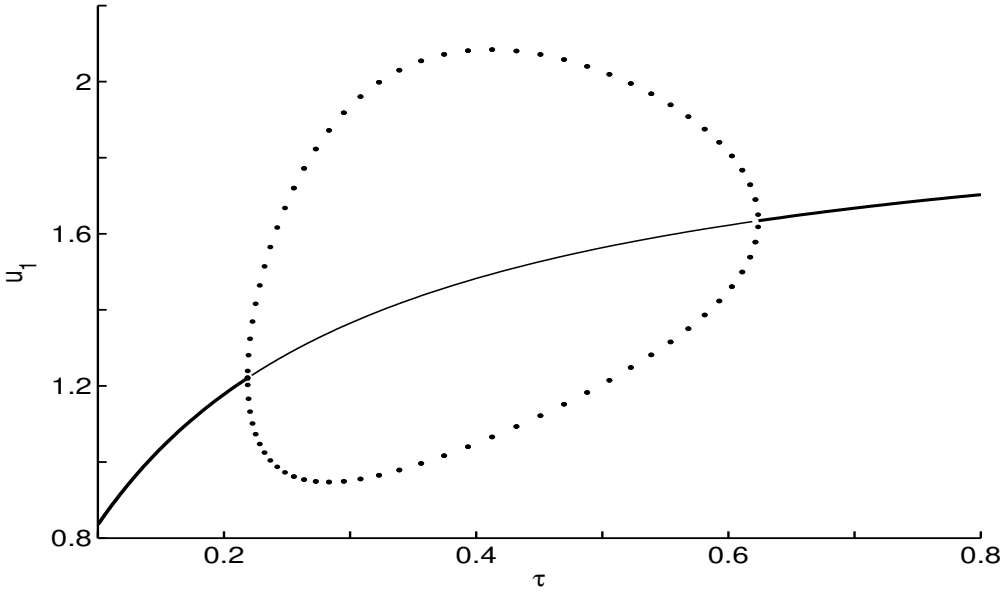

Caption: Global solution branches u_{1e} versus τ for $m = 5$ cells: Heavy (thin) solid is stable (unstable) steady-steady. Dots indicate stable periodic solution branch. HB points at $\tau_{H-} = 0.2187$ and $\tau_{H+} = 0.6238$.

Key: Stable synchronous oscillations occur in some τ interval. Limiting well-mixed ODE dynamics is independent of cell locations and D.

Quorum sensing (Qualitative): Collective behavior of "cells" in response to changes in their population size. There is a threshold number m_c of cells or a critical cell density ρ that is needed to initiate a collective behavior.

Quorum sensing (Math): For what range of m, do the well-mixed ODEs have a stable periodic solution on $\tau_{H-} < \tau < \tau_{H+}$ with HB points at $\tau_{H\pm}$?

Quorum Sensing Behavior

What parameters control control QS behavior? We will study QS behavior as the permeability d_1 is varied and $d_2 = 0.2$: Recall:

$$\partial_{n_j} U = d_1 U - d_2 u_j^1 \,, \qquad \text{on} \quad \partial\Omega_{\varepsilon_j} \,, \quad j = 1, \ldots, m \,.$$

Remark: Equivalent to finding the range of m for which the instability lobe for the synchronous mode is unbounded in the τ versus D plane.

Left: Quorum threshold m_c vs. d_1 from ODEs. Right: τ vs. D for $d_1 = 0.3$, $r_0 = 0.5$.

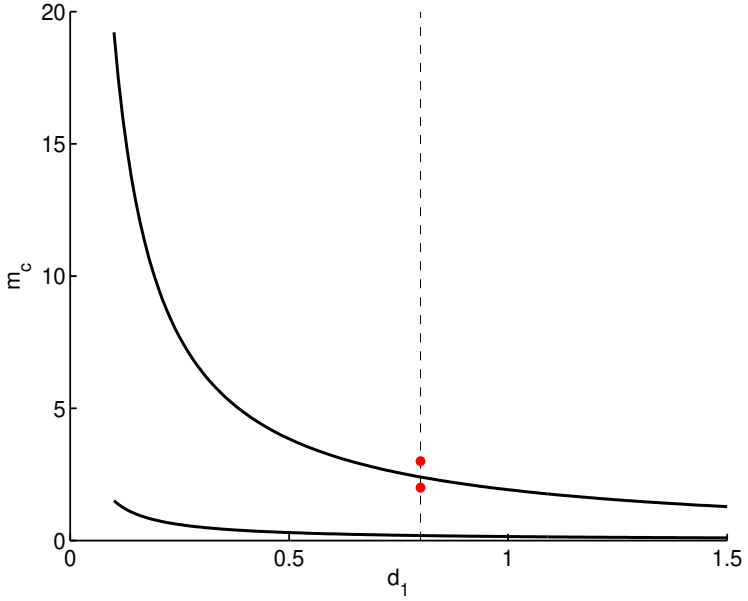

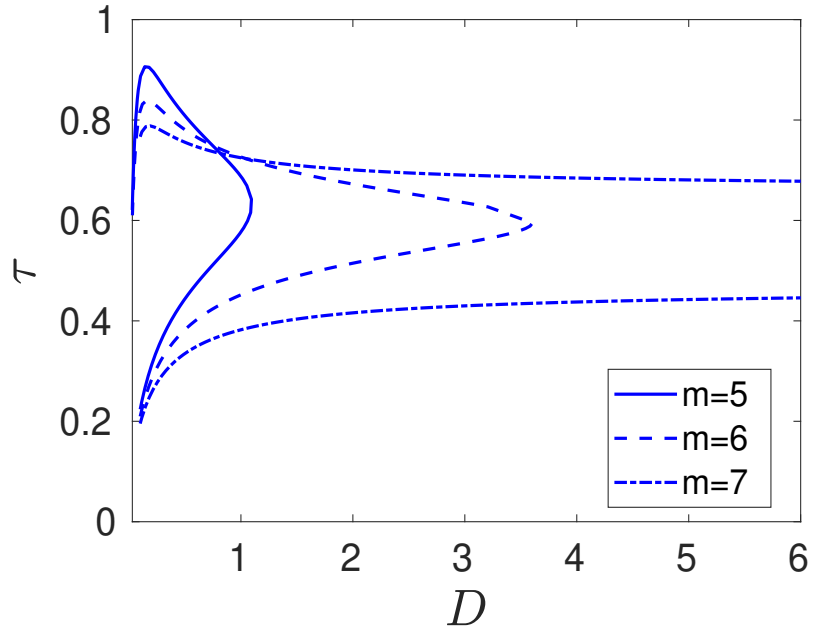

Key: m_c sensitive to small changes in d_1

$d_1 = 0.8\,, m_c = 3\,;$ $d_1 = 0.3\,, m_c = 7\,;$ $d_1 = 0.2\,, m_c = 12\,;$ $d_1 = 0.1\,, m_c = 19\,.$

Large Cell Populations: Synchronization I

In the well-mixed limit $D \to \infty$, the PDE-ODE system reduces to

$$U_0' = -\frac{1}{\tau} U_0 - \frac{\rho}{m\tau} \sum_{j=1}^{m} \left[\kappa_{1,j} U_0 - \kappa_{2,j} u_j^1 \right] ,$$

$$\boldsymbol{u}_j' = \boldsymbol{F}_j(\boldsymbol{u}_j) + \frac{1}{\tau} \left[\kappa_{1,j} U_0 - \kappa_{2,j} u_j^1 \right] \boldsymbol{e}_1 , \qquad j = 1, \ldots, m ,$$

where $\rho = m/|\Omega|$ is the "cell density" $\kappa_{1,j} \equiv 2\pi d_{1,j}$ and $\kappa_{2,j} \equiv 2\pi d_{2,j}$.

Non-Identical Cells: We take $\tau = 0.5$, and fix common permeability parameters $d_{1j} = 0.8$ and $d_{2j} = 0.2 \ \forall j$. The intracellular kinetics $\boldsymbol{F}_j$ are not identical. Selkov parameters $\varepsilon_0 = 0.15$ and $\mu = 2$ are fixed for each cell, but α can vary from cell to cell. Isolated cells are not oscillatory.

Kuramoto order parameter: (measures the degree of oscillator phase synchrony):

$$R = \left\langle \left| N^{-1} \sum_{j=1}^{N} \exp[i\theta_j(t)] - \left\langle N^{-1} \sum_{j=1}^{N} \exp[i\theta_j(t)] \right\rangle \right| \right\rangle , \quad 0 \le R \le 1 .$$

$R = 1$ (Perfect phase synchrony); $R = 0$ (No phase coherence);

Large Cell Populations: Synchronization II

Computations of order parameter R with respect to ρ. Iyaniwura (UBC)

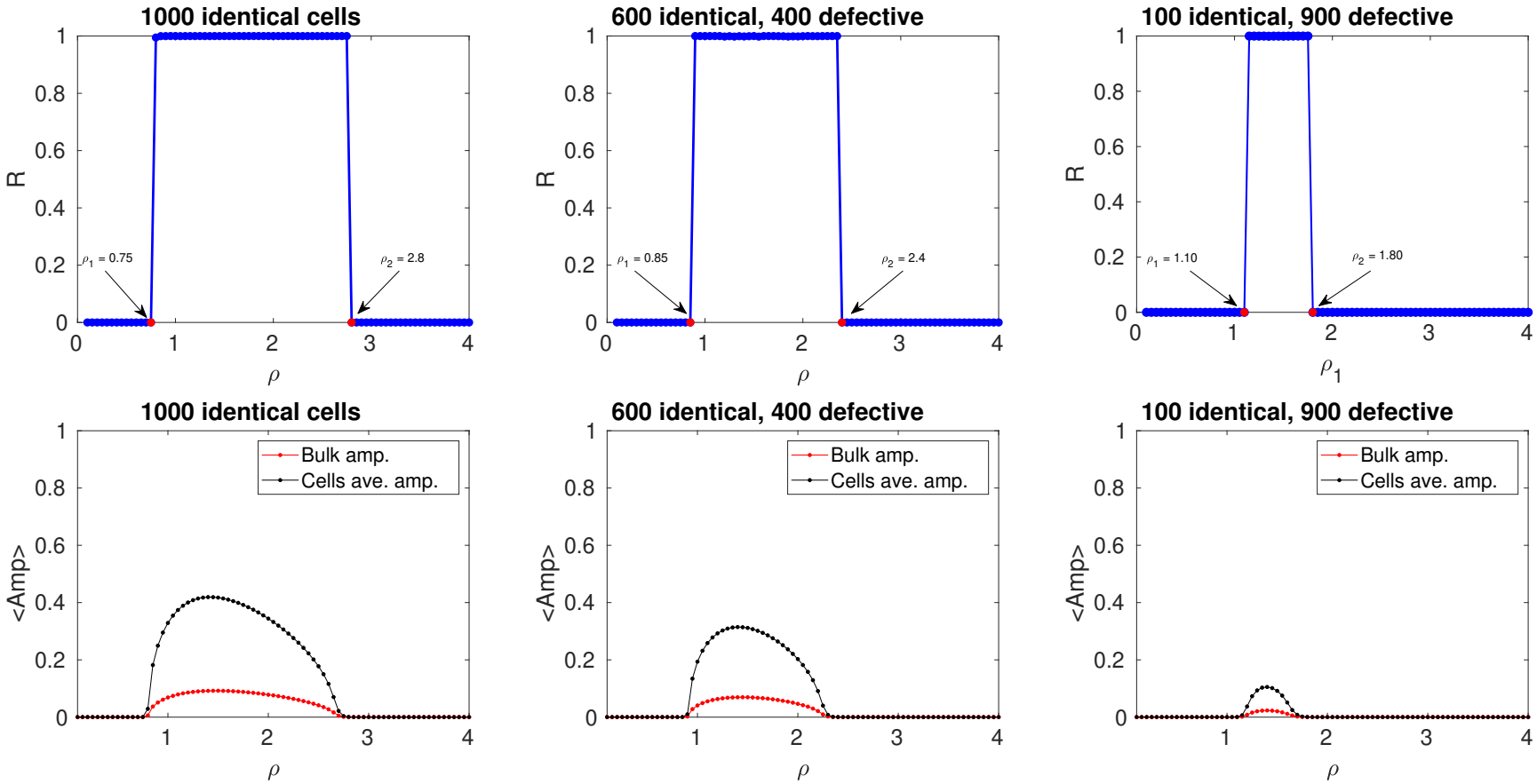

- Identical cells: $\alpha = 0.9$. "Defective" cells: α is random in $0.921 \leq \alpha \leq 0.952$.
- Population density ρ plays a dual role of triggering and quenching oscillations
- Interval of ρ where synchrony occurs decreases as the number of defective cells increases.

Cell-Bulk Model: Further Directions

Let $D = \mathcal{O}(1)$. Consider m "randomly" placed cells in a disk. Can we observe clusters of oscillating and non-oscillating cells? (i.e. "chimera"-type states.)

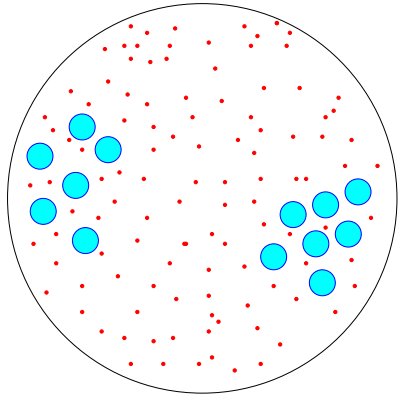

- How do we solve the spectral problem in arbitrary domains? (fast multipole methods for G and G_λ)
- Numerics for the GCEP for large numbers of cells.
- What if the steady-state solution is not unique (hysteresis) or if intracellular dynamics has a time-delay?
- Intracellular dynamics to model a specific biological system (LuxIR circuit in *Vibrio fischeri*).
- Derive a RD system in the homogenized limit of $m \gg 1$ but $m\epsilon^2 \ll 1$.
- Two bulk-diffusing (autoinducer) species.
- PDE-ODE Model in 3-D. (interactions are, in general, much weaker owing to $1/r$ decay of Green's function).

PDE-ODE Cell-Bulk Model in 3-D

The dimensionless bulk concentration $U(\mathbf{x},t)$ satisfies

$$\frac{\partial U}{\partial t} = D\,\Delta U - \kappa\, U, \quad \mathbf{x}\in\Omega\setminus\cup_{j=1}^{m}\Omega_{\varepsilon_j}\,; \quad \partial_n U = 0, \quad \mathbf{x}\in\partial\Omega\,,$$

$$\varepsilon D\,\partial_n U = d_{1,j}\,U - \frac{d_{2,j}}{\varepsilon}u_j^1\,, \quad \mathbf{x}\in\partial\Omega_{\varepsilon_j}\,, \quad j=1,\ldots,m,$$

which is coupled to the dimensionless intracellular dynamics for the j^{th} cell

$$\frac{d\boldsymbol{u}_j}{dt} = \boldsymbol{F}_j\left(\boldsymbol{u}_j\right) + \boldsymbol{e}_1\int_{\partial\Omega_{\varepsilon_j}}\left(\frac{d_{1,j}}{\varepsilon}U - \frac{d_{2,j}}{\varepsilon^2}u_j^1\right)dS\,, \quad j=1,2,\ldots,m,$$

where $\boldsymbol{u}_j=(u_j^1,\ldots,u_j^n)^T$, $\boldsymbol{e}_1\equiv(1,0,...,0)^T$, and $d_{2,j}=\mathcal{O}(1)$.

Near Well-Mixed Limit: An interesting limit where there is $\mathcal{O}(1)$ interaction between the cells is when

- $D=\mathcal{O}(\varepsilon^{-1})$, $\kappa=\mathcal{O}(1)$, $d_{1,j}=\frac{\widetilde{d}_{1,j}}{\varepsilon}$, where $\widetilde{d}_{1,j}=\mathcal{O}(1)$.
- In this regime, Quorum and Diffusing sensing can be studied through a common limiting system.

ODE System in Near Well-Mixed Limit

In this limit, the PDE-ODE system reduces to

$$U_0' = -\kappa\, U_0 + \frac{4\pi}{|\Omega|}\sum_{j=1}^{m}(p_{2,j}\, v_j^1 - p_{1,j}\, U_0) - \frac{16\pi^2\varepsilon}{|\Omega|}\sum_{j=1}^{m} p_{1,j}\,(\mathcal{G}\,\boldsymbol{c})_j + \dots\,,$$

$$\frac{d\boldsymbol{v}_j}{dt} = \boldsymbol{F}_j\,(\boldsymbol{v}_j) + 4\pi\boldsymbol{e}_1(p_{1,j}U_0 - p_{2,j}v_j^1) + 16\varepsilon\pi^2\,\boldsymbol{e}_1\,p_{1,j}(\mathcal{G}\,\boldsymbol{c})_j + \dots\,,\quad j = 1,\dots,m\,,$$

where $\boldsymbol{c} = (c_1,\dots,c_m)^T$, $\mathcal{G}$ is Neumann Green's matrix in 3-D and

$$p_{1,j} \equiv \frac{D_0\,\widetilde{d}_{1,j}}{\widetilde{d}_{1,j} + D_0}\,,\quad p_{2,j} \equiv \frac{D_0\,d_{2,j}}{\widetilde{d}_{1,j} + D_0}\,,\quad c_j \equiv \frac{d_{2,j}v_j^1 - \widetilde{d}_{1,j}U_0}{\widetilde{d}_{1,j} + D_0}\,,\quad j = 1,\dots,m\,.$$

- For $D_0 \to 0$, then $p_{1,j} \to 0$ and $p_{2,j} \to 0$ (no cell-cell communication).
- For $D_0 \to \infty$ (well-mixed), then $p_{1,j} \to \widetilde{d}_{i,j}$, $p_{2,j} \to d_{2,j}$, and $c_j \to 0$ (maximal cell-cell communication, but cell configuration insignificant).
- For $D_0 = \mathcal{O}(1)$ dependence on cell configuration and shape of confining domain Ω is at $\mathcal{O}(\varepsilon)$ term through Neumann G-matrix $\mathcal{G}$.
- ODE system: reveals both quorum sensing and diffusion sensing behavior.